

Using Hydrogeomorphic Features to Quantify Structural and Functional Hydrologic Connectivity in a Coastal Plain Headwater Stream

Delaney M. Peterson¹, C. Nathan Jones¹, Alain M. Plattner², Ariel J. Shogren¹, and Sarah E. Godsey³

¹Department of Biological Sciences, University of Alabama, Tuscaloosa, AL, USA.

²Department of Geological Sciences, University of Alabama, Tuscaloosa, AL, USA.

³Department of Geosciences, Idaho State University, Pocatello, ID, USA.

Corresponding author: Delaney Peterson (dmpeterson2@crimson.edu)

Author ORCIDs:

Peterson: 0000-0002-3444-4772

Jones: 0000-0002-5804-0510

Plattner: 0000-0001-5154-1833

Shogren: 0000-0002-1284-3836

Godsey: 0000-0001-6529-7886

This is a non-peer-reviewed manuscript being submitted to Water Resources Research.

Key Points:

- Hydrogeomorphic features provide a new framework to study streamflow generation along the river corridor.
- Across the study watershed, hydrogeomorphic features demonstrated distinct patterns of groundwater-surface water connectivity.
- Within hydrogeomorphic features, spatial variability in clay confining layers led to temporal variability in perched flowpath activation.

Abstract

Headwater streams comprise most of the global river length, and hydrologic processes occurring in headwaters affect the chemical, physical, and biological functions of downstream aquatic ecosystems. However, we do not have a clear understanding of the spatial scales that drive hydrologic processes across headwater systems, particularly in Coastal Plain landscapes. We address this gap by characterizing hydrologic connectivity in a small, forested watershed in the Coastal Plain of Alabama, USA. We collected data across three spatial scales: the watershed (0.9 km²), hydrogeomorphic feature (100-500 m), and hillslope (10-100 m) scales. We characterized stream network variability using seasonal surveys combined with water monitoring wells to characterize stream hydrologic state across 2021, paired with an Electrical Resistivity Tomography (ERT) and Time Domain Induced Polarization (TDIP) survey to characterize subsurface structure. Our results suggest that discretizing the river corridor into distinct hydrogeomorphic features provides a framework for understanding the dynamics of hydrologic connectivity within a watershed. Each hydrogeomorphic feature experienced consistent hydrologic states that differ along the network: incised channels gained water, intact riparian zones lost water, and wetland-stream complexes reflected no net water gain or loss from the river corridor. Subsurface structures observed with the ERT/TDIP survey indicate heterogeneous perched flowpaths, with saturation occurring variably throughout both space and time. Altogether, these results suggest that studying watersheds across a hierarchy of scales can provide insight into the dynamics of hydrologic connectivity, and that hydrogeomorphic features can provide a key intermediate scale for the integration of hydrologic processes across the river corridor.

Plain Language Summary

Small streams are vitally important water resources; they provide flood protection, important habitat for amphibians and fish, and often drinking water for downstream communities.

However, small streams are incredibly variable, and it is unclear whether we need to study every hillslope, valley, or watershed to predict how small streams impact downstream areas. We address this knowledge gap by quantifying hydrologic connectivity – or the water-mediated movement of materials, energy, and organisms – across a watershed located in the southeastern US. We collected data across three spatial scales: the largest watershed scale (0.9 km²), the intermediate scale we define as the hydrogeomorphic feature (100-500 m), and the smallest hillslope scale (10-100 m). Our data suggest that splitting watersheds into separate hydrogeomorphic features that are defined by the shape of their valley provides a framework for understanding hydrologic connectivity in small streams. As an example, we found incised streams typically received water from surrounding hillslopes, whereas streams without incision typically lost water to the surrounding hillslope. Additionally, subsurface imaging suggests that patchy clay soils play an important role in the movement of water. Together, these results suggest that studying watershed across scales can help us understand how small streams impact downstream areas.

1 Introduction

Headwater streams comprise over 80% of global river networks (Downing et al., 2012), and are defined as low-order (i.e., 1st-3rd Strahler order, Vannote et al., 1980) streams that occupy the upper reaches of stream networks (Nadeau & Rains, 2007). Headwaters are important hydrologic features with unique physical (Alexander et al., 2007; Allen et al., 2018), chemical (Alexander et al., 2007; Peterson et al., 2001), and biological (Meyer et al., 2007; Richardson & Danehy, 2007) downstream impacts, and represent the dynamic interface between terrestrial hillslopes and aquatic ecosystems (Gomi et al., 2002; Lowe & Likens, 2005). However, most studies have focused on headwaters as low-order perennial streams mapped at the 1:100,000 scale (Doyle & Ensign, 2009; Nadeau & Rains, 2007), which often excludes the field-observable but difficult-to-map non-perennial and zero-order channels that feed downstream, mapped headwaters (Gomi et al., 2002; Shanafield et al., 2021). In many humid systems, most non-perennial stream reaches are found in the headwaters of stream networks (Costigan et al., 2016;

Nadeau & Rains, 2007; Shanafield et al., 2021). Therefore, headwater systems are typically conceptualized such that perennial flow occurs where the permanent water table intersects with the hillslope, and all channels upstream of this point only flow when seasonal water table fluctuations intersect (Dunne & Black, 1970; Hewlett & Hibbert, 1967; Winter, 1999; Zimmer & McGlynn, 2017).

Heterogeneity in the subsurface can result in streamflow generation and network dynamics that do not align with these previous conceptualizations. Preferential flow, or non-equilibrium flow, is the process by which infiltrating water and solutes are channelized into a small fraction of the available pore space in the subsurface (Jarvis et al., 2016). Perched flowpaths are a form of preferential flow that are driven by confining layers and soil horizons with contrasting hydraulic conductivities (Baird & Low, 2022; Nimmo, 2012; Weyman, 1973), and can lead to heterogeneity in subsurface saturation (e.g., shallow, transient, perched water tables; Zimmer & McGlynn, 2017). However, the aforementioned conceptualizations of network structure and streamflow generation rely on a continuous saturated water table that intersects with the ground surface at all points downstream of a channel head (Winter, 1999). Therefore, heterogeneity and discontinuity in subsurface saturation introduced by perched flowpaths can result in transient flows and network disconnection downstream of the channel head.

Hydrologic variability and streamflow generation are controlled by hierarchical drivers, or drivers that interact predictably across scales (*sensu* Jencso & McGlynn, 2011). One of the foundational conceptualizations of the hierarchical drivers of flow in headwater streams is the Variable Source Area concept (Hewlett & Hibbert, 1967). This defined the drivers of network expansion and contraction in small humid-climate watersheds as primarily depth to impervious layers and similar soil characteristics, followed by watershed slope and topographic characteristics, then climatic factors like the magnitude and frequency of storm events, and lastly land use (Hewlett & Hibbert, 1967). Others have built upon this conceptualization by studying hydrologic processes across spatial scales from the soil grain, plot, reach, to watershed, and have found that watershed physiographic variables (i.e., geology, topography, soil structure) and land use also emerge as drivers of streamflow generation (Costigan et al., 2016; Jencso et al., 2009; McGuire et al., 2005; Prancevic & Kirchner, 2019; Spence, 2010; Trancoso et al., 2017; Warix et al., 2023). However, there are challenges to integrating across spatial scales to better understand

drivers and processes. For example, spatial heterogeneity and threshold behavior span gradients of time and space, such that data collected at smaller scales might not represent the larger patterns that emerge within an entire watershed (Jencso et al., 2009; McDonnell et al., 2007). Further, streamflow generation processes do not organize into measurable scales, but rather integrate across all subordinate scales with respect to connectivity and heterogeneity, resulting in catchments responding differently to the same factors (Spence, 2010). Therefore, it is difficult to predict how, when, and where these well-documented hierarchical drivers interact across scales to influence streamflow generation, and we are still looking for effective scales and methods of study to elucidate the processes that drive the emergent patterns of streamflow generation.

Hydrologic connectivity represents a conceptual framework that has the potential to unify concepts from across disciplines and spatial scales (Jones et al., 2019). Hydrologic connectivity is broadly defined as the water-mediated movement of materials, organisms, and energy between watershed components (Pringle, 2001; Rinderer et al., 2018), and provides a unifying concept that can be used to integrate the importance of water fluxes across disciplines (i.e., ecology, biogeochemistry, geomorphology, and hydrology; Jones et al., 2019; Larsen et al., 2012). Hydrologic connectivity is often measured as the magnitude, frequency, duration, and intensity of hydrologic exchange flows (Covino, 2017; Harvey & Gooseff, 2015), often across three spatial dimensions (vertical, lateral, and longitudinal) and time (Ward, 1989; Zimmer & McGlynn, 2018). Hydrologic connectivity can also be conceptualized through the lens of structural and functional connectivity (Bracken et al., 2013). Here, structural connectivity is the physical adjacency of watershed components that would allow connectivity. Functional connectivity is the resulting flux of water, solutes, and organisms (Larsen et al., 2012; Rinderer et al., 2018). However, there is no universal measure or metric of connectivity, and there has been no uniform dimension or scale of study that has been employed across all systems.

Across the hydrologic sciences, there are multiple research frameworks and associated communities of researchers working to predict drivers of streamflow generation and subsequent network dynamics. However, they focus on different and distinct spatiotemporal scales such that they may capture emergent properties rather than primary drivers. Hydrogeomorphology has been loosely defined as an interdisciplinary research area focused on the complex interactions between geomorphology and hydrology to understand aquatic ecosystems (Poole, 2010; Sidle &

Onda, 2004). Therefore, hydrogeomorphology generally combines geomorphic principles (e.g., sediment regimes and channel bedform dynamics) with hydrologic principles (e.g., hydrologic fluxes and stream network dynamics) to characterize the physical template of systems. Alternatively, river corridor science is a recent area of study focused on hydrologic connectivity and riparian-stream corridor processes (Harvey & Gooseff, 2015). While initially focused on near-stream exchange flows at scales smaller than river reaches (e.g., geomorphic bedforms, Cardenas et al., 2004), river corridor science also aims to understand how hillslope and upland processes influence exchange flows in the river corridor (Harvey & Gooseff, 2015; Wymore et al., 2023). Finally, the network dynamics community has recently focused on using stochastic network modeling to understand the patterns and processes of stream network expansion and contraction (e.g., Aho et al., 2023; Botter & Durighetto, 2020; Prancevic & Kirchner, 2019). These studies utilize a perceptual model of hierarchical and stable drivers of wetting or drying at points within the network to investigate the potential drivers of connectivity dynamics at the network scale.

The spatial scales of these three study areas are disconnected. Hydrogeomorphic research has focused on primarily reach and network scales (100 to 10^{10} m, Grabowski & Gurnell, 2016; Poole, 2010). River corridor science has focused on either patterns at the largest (10^4 to 10^7 m, Wymore et al., 2023) or processes at the smallest (sub-10 m, Harvey & Gooseff, 2015) scales. Network dynamics research has focused on temporally static patterns at the network scale (e.g., Botter & Durighetto, 2020; Prancevic & Kirchner, 2019). These research areas lack a clear intermediate scale of study that would allow for the study of both nested and emergent processes. Therefore, we propose that hydrogeomorphic features (on the order of 100 to 1,000 m) can be used as that intermediate scale to study river corridor processes across the hydrogeomorphic continuum.

In this study, we quantify hydrologic connectivity across spatial scales to elucidate drivers of streamflow generation in a low-gradient, understudied headwater system. Our research objectives include (i) to propose an intermediate spatial scale (here, hydrogeomorphic features) that would allow us to integrate our understanding of structural connectivity across the entire river corridor; (ii) to examine differences in hydrologic connectivity across hydrogeomorphic

features in our study watershed; and (iii) to document within-hydrogeomorphic feature heterogeneity using differences in structural and functional connectivity across the river corridor.

2 Materials and Methods

Our study characterizes hydrologic connectivity across three distinct spatial scales in a Coastal Plain headwater stream over the span of one calendar year (2021). At the coarsest watershed scale, we characterized hydrologic connectivity using geospatial data and seasonal stream network surveys to identify the active surface drainage network (ASDN). At the intermediate hydrogeomorphic feature scale, we characterized hydrologic connectivity using a combination of geospatial analysis and network of groundwater and surface water monitoring wells. Finally, at the finest hillslope scale, we characterized hydrologic connectivity using soil surveys, nested groundwater monitoring wells, and geophysical measurements.

2.1 Site Description

The Coastal Plain represents a largely understudied region, despite comprising over 1.1 million km² (>14%) of the continental US and representing a system with diverse hierarchical drivers of streamflow generation. The Coastal Plain presents a unique physical template that will inform our understanding of how water moves through landscapes and challenge existing geographically-derived paradigms (Burt & McDonnell, 2015). Generally, landscapes organize into erosion-, transport-, and deposition-dominated zones based on topographic gradients (Jaeger et al., 2017; Schumm, 1977). The presence and severity of these zones can be further exacerbated by the land-use legacies that dominate the landscape; in the southeastern USA specifically, land management decisions have resulted in consequences for forest community composition, soil structure, and stream channel structure and incision (Foster et al., 2003; Galang et al., 2007; Maloney et al., 2008). While recent research has expanded into lower-gradient systems (e.g., Tetzlaff et al., 2011; Zimmer & McGlynn, 2017), and coastal alluvial plains (e.g., Epps et al., 2013; Lee et al., 2023), this physiographic province represents a key region where more work is needed.

We conducted this study in a 0.9 km² low-gradient watershed located at the Tanglewood Biological Station in Hale County, AL (USA, Figure 1a) from January 1 to December 31, 2021.

The region has a humid subtropical climate and receives an average of 1,390 mm of precipitation per year as almost entirely rainfall (NOAA National Centers for Environmental information, 2023). In 2021, the annual precipitation was slightly above average with the area receiving 1,470 mm, 50% of which fell between June and September. Tanglewood has a mean annual temperature of 17.6°C and a watershed-aggregated mean annual evapotranspiration of 986mm (Running et al., 2021)

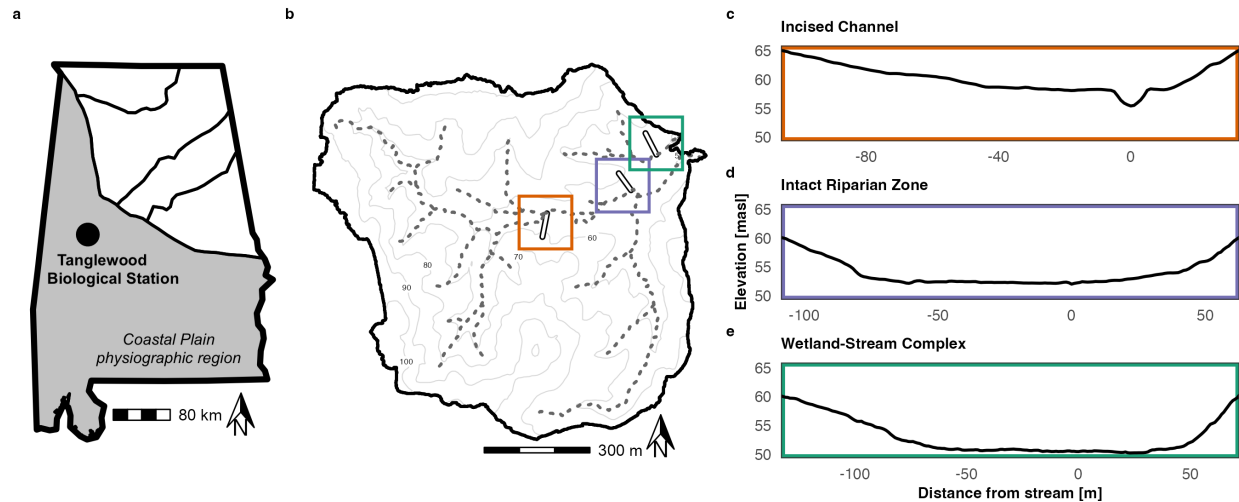


Figure 1. (a) a map of Alabama showing the physiographic provinces of the southeastern US, with the Coastal Plain highlighted in grey, and the Tanglewood Biological Station indicated with a black point. (b) the 0.9 km² study watershed at the Tanglewood Biological Station, with elevation bands indicated in light grey and the stream network delineated by the grey dashed line. The groundwater well transects are shown as hollow black segments perpendicular to the stream network and are highlighted by boxes colored according to their respective hydrogeomorphic feature, which correspond to the valley cross-sections in (c), (d), and (e). Additionally, one ERT/TDIP transect was performed along the well transect in the wetland-stream complex hydrogeomorphic feature. (c) is a 200 m valley cross-section of the incised channel hydrogeomorphic feature, showing the distinct channel incision and narrow valley bottom. (d) is a 200 m valley cross-section of the intact riparian zone hydrogeomorphic feature, showing the wider U-shaped valley bottom and less-incised channels. (e) is a 200 m valley cross-

section of the wetland-stream complex, showing the wide U-shaped and low-gradient valley bottom.

Physiographically, this site is in the Coastal Plain province and exists within the larger East Gulf Coastal Plain physiographic section (Figure 1a, Kidd & Lambeth, 1995, Osborne et al., 1989). The site is located in the Fall Line Hills district of the province, which is characterized by low-gradient sandy upland areas dissected by severely entrenched streams (Kidd & Lambeth, 1995). Geologically, the region is comprised of units of sedimentary origin, with approximately 1,000-foot-thick unconsolidated Mesozoic and Cenozoic sediments that overlay lower-Cretaceous and pre-Cretaceous sedimentary rocks from adjacent physiographic provinces (Davis, 1988; Osborne et al., 1988; Raymond et al., 1988). Upland areas are primarily high terrace deposits that can be as much as 100 feet thick (Kidd & Lambeth, 1995), and are underlain by the Eutaw Formation and Tuscaloosa Group geologic units (Osborne et al., 1988, 1989). Geomorphically, the region is low- to moderate-gradient, with greater relief occurring in stream valleys (Raymond et al., 1988). The unconsolidated sediments are primarily composed of gravels, sands, silts, and clays, and result in deep, highly weathered soils with structured horizons (Alabama Cooperative Extension System, 2018; Neilson, 2007; Kidd & Lambeth, 1995). The soils are primarily well-drained ultisols with argillic confining horizons; dominant soil series include Luverne-Smithdale complexes as well as the Lucedale, Bama, Mantachie Kinston and Iuka, and Savannah soil series (Soil Survey Staff, n.d.). Hydrologically, the Tanglewood Biological Station drains an unnamed tributary of Fivemile Creek, which is in the larger Black Warrior River and Mobile Bay basins.

In this region, geomorphology and climate interact to create distinctive low-gradient headwater systems. Tanglewood, like many headwater systems in the region, has highly erodible soils that interact with past agricultural land uses and high subsurface water storage capacities to form highly dendritic and dense network structures with distinct hydrogeomorphic features (Figure 1c-e). Here, we defined hydrogeomorphic features as distinct geomorphic features such as valley shape, ridges and swales, gullies, and incised channels that are both formed by and contribute to hydrologic patterns such as hydrologic state and water table lowering.

For the purposes of this study, we identified three distinct hydrogeomorphic features in our watershed: (1) erosion-dominated incised channels (Figure 1c), (2) transport-dominated intact riparian zones (Figure 1d), and (3) deposition-dominated wetland-stream complexes (Figure 1e). These hydrogeomorphic features occurred in a predictable order across short stream distances, with incised channels occurring in high-gradient areas that flow into sections of the river corridor with intact riparian zones, and then downstream, zones with sediment deposition that form wetland-stream complexes occur at low-gradient slope breaks. Incised channels were defined here as > 0.5 m of incision between the streambed and banks. Incised channels often had relatively stable banks, with no clear evidence of mass wasting events throughout the study period; they often initiated at obvious channel heads that formed at knickpoints in clay soil horizons or vegetative structures. Intact riparian zones were defined here as sections of the river corridor with clear bed-and-bank structure that were incised < 0.5 m and were predominantly composed of sandy substrate with wide riparian zones. Wetland-stream complexes were defined here as sections of the river corridor where low slope gradients created anastomosing streams between riparian wetlands and had large depositional areas for sediment and organic matter with highly organic riparian soils. These structural differences in hydrogeomorphology reflect a variety of water, sediment, and landscape processes interacting across space and time.

2.2 Characterizing Hydrologic Connectivity

We measured watershed-scale patterns of hydrologic connectivity with stream network ASDN surveys. We measured hydrogeomorphic feature-scale patterns of hydrologic connectivity using water table elevation gradients as a proxy for groundwater-surface water interactions. We observed patterns of hydrologic connectivity at the hillslope-scale with the presence or absence of water in nested wells. To characterize groundwater-surface water connectivity, we deployed a nested series of 14 monitoring wells instrumented with HOBO U20L-04 pressure transducers. We performed all data processing and geospatial analyses with R version 4.0.3 (2020-10-10, R Core Team, 2023) using the *whitebox* (Wu & Brown, 2022), *sf* (Pebesma, 2018), and *raster* (Hijmans, 2023) packages.

2.2.1 Watershed Scale

At the watershed scale, we measured ASDN expansion and contraction using seasonal network surveys as a proxy for longitudinal connectivity (*sensu* Zimmer & McGlynn, 2018). We assigned 78 sites throughout the geomorphic stream network (defined here as a geomorphic channel free of vegetation that is > 10 cm in width), placing sites approximately 100 m apart as well as downstream of every confluence. We then visited every site in January, May, August, and November 2021 to capture conditions during each of the primary climatological seasons. At each site, we measured presence or absence of water, wetted channel width, and visually estimated the percent of surface water connectedness between sites. Notably, there were several locations where surface water was assumed to be routed through subsurface macropores (e.g., Figure 2D from Wilson et al., 2013, Figure 1 from Samad et al., 2023). We marked these locations as disconnected with water absent due to the lack of surface flow. We conducted these surveys in a single day at baseflow conditions, which we assumed to be representative of seasonal baseflow conditions. We only used 51 sites for our network analyses, as we never observed flow at 27 of the original 78 sites. We determined that these sites could be defined as ephemeral, and thus not representative of baseflow conditions.

We estimated the total network ASDN length for the watershed using the *wbt_distance_to_outlet* function in *whitebox* (Wu & Brown, 2022). Using a 1 m resolution Digital Elevation Model (DEM; National Digital Elevation Program, 2021), we first processed the DEM to remove pits and gaps. We then used *wbt_d8_pointer()* and *wbt_d8_flow_accumulation()* to generate a flow direction and flow accumulation raster, respectively (Wu & Brown, 2022). We then delineated the geomorphic channel network using a flow accumulation threshold that most closely resembled field observations (here, 2,500 1 m pixels) to calculate the maximum potential ASDN extent. Then, we calculated ASDN length for each survey as stream distance between two sites multiplied by the percent connectedness observed per survey and aggregated to a total wetted network length.

2.2.2 Hydrogeomorphic Feature Scale

To capture patterns across hydrogeomorphic features, we delineated the hydrogeomorphic features according to channel and valley topographic metrics. We delineated

hydrogeomorphic features using 20 m-long valley cross-sections centered at the thalweg and oriented orthogonal to the channel at each of the 78 ASDN sites. We then calculated a suite of topographic metrics across those cross-sections, including average near-channel slope, maximum change in elevation across the stream channel, and channel width-depth ratio. Incised channel sites were defined as cross-sections with a width-depth ratio < 15 and a maximum near-channel elevation change > 0.5 m. We defined wetland-stream complex sites as cross-sections with width-depth ratios > 25 . We defined intact riparian zone sites as cross-sections falling between incised channel and wetland-stream complex criteria. We then compared our calculated hydrogeomorphic features to field observations to confirm delineations, which were accurate for 83% of sites.

Then, we installed one well transect in each of our delineated hydrogeomorphic features to measure the hydrologic state of the stream as a proxy for lateral connectivity (*sensu* Zimmer & McGlynn, 2018). We operationalized hydrologic state as the elevation gradient of the saturated water table that would indicate gain, loss, or equilibrium of the groundwater and surface water. We installed well transects perpendicular to the stream in locations that best reflected the local topography. Each transect consisted of one shallow (< 2 m) in-stream stilling well, one deep (> 2 m) floodplain well, one set of nested wells in the lower hillslope at the transition from riparian to upland vegetation, and one deep well in the upper hillslope (Figure S1). We hand-augered all wells to depths of refusal, and soils were characterized visually by structure, color, and texture during installation. We installed all wells such that they were screened from depths of refusal to 10 cm below the soil surface, and nested deep wells were screened from depths of refusal to the depth of the identified argillic confining horizon ($B_{t_{gx}}$). We instrumented wells with unvented pressure transducers recording at synchronous 15-minute intervals from January 1 to December 31, 2021. We converted gage pressure to water level (m) by correcting with a nearby barometric pressure transducer and the specific weight of water. We converted water level for each well to water table elevation (meters above sea level, hereafter masl) using surveyed elevation data. We then divided these water elevations by linear surface distance between the wells (m) to calculate water table slope (m/m) between every set of wells, which was used to calculate hydrologic state.

2.2.3 Hillslope Scale

To characterize variability of hydrologic connectivity within hydrogeomorphic features, we used nested wells and soil characteristics to measure the ability for water to move between shallow and deeper subsurface layers. As this operationalized connectivity is a function of subsurface structure, we characterized soils using structure, color, and texture from boreholes used for well installation depths. We delineated horizon depths from the soil removed from the borehole, and which were corrected to the total depth of the borehole by multiplying horizon depth by the quotient of the measured soil profile length and the borehole depth. We then converted these horizon depths to elevations using surveyed data to be compared to water elevation data (Table S1).

We installed nested wells in locations where there were identified argillic confining layers that would impede water movement (in this case, the lower hillslope position of both the incised channel and wetland-stream complex transects). Boreholes without confining layers shallower than 4 m were considered locations of high vertical connectivity and were excluded from this analysis. We installed nested wells such that the deep well was screened from the confining layer to the depth of auger refusal, and the shallow well was screened from 10 cm below the ground surface to that confining layer (Figure S1). We instrumented these wells with pressure transducers recording at synchronous 15-minute intervals from January 1 to December 31, 2021. This resulted in the ability to detect when a perched saturated layer formed above the confining layer, as the water level in the shallow well would be closer to the surface than the water level in the deeper well. We converted water level to water elevation (masl) using surveyed elevation data, which was further aggregated to daily presence/absence of a saturated water table in each well.

To add further context and characterization of subsurface structure and to extrapolate soil horizons beyond the boreholes, we conducted an electrical resistivity tomography (ERT) survey including direct current and time domain-induced polarization (TDIP) measurements on one transect in the wetland-stream complex hydrogeomorphic feature. We collected these data in September 2021 during dry conditions to reduce the effect of water on the measurements. We used an ABEM Terrameter LS2 system with 48 electrodes and four channels. Our electrode

arrays and electrical current waveform used dipole-dipole measurements as well as a multichannel version of the Wenner array (following Plattner et al., 2022). The electrical current waveform consisted of a 4 s on cycle followed by a 4 s off cycle, during which measurements of the decaying electrical potential were taken at 14 timestamps, the earliest of which was after 10 ms post current shutoff and the last after 3.4 s post current shutoff. We used the roll-along method (*sensu* Loke et al., 2013) to extend our transect. In the riparian floodplain, the electrodes were spaced 0.5 m apart. On the hillslope, we increased the electrode spacing to 1 m.

We removed measurements for which the electrical potentials did not decay over time post current shutoff. We also removed measurements for which the apparent electrical resistivity calculated from the injected current and measured potential difference was an obvious outlier, defined as an apparent electrical resistivity less than 30 Ohm m or greater than 900 Ohm m. In total, we collected measurements for 1336 electrode combinations, of which we rejected 95. From the remaining measurements, we inverted for a resistivity profile as well as for chargeability profiles for each time step using the open-source software GIMLi (Rücker et al., 2017). From the chargeability profiles at each time step, we calculated the chargeability profile at shutoff time by fitting a time-domain Cole-Cole model (Yuval & Oldenburg, 1997) for each subsurface cell. To remove the dependence of the chargeability on the resistivity, we calculated the normalized chargeability, which is defined as the ratio between the chargeability and the resistivity and provides a substantially improved measure for clay content (Slater & Lesmes, 2002).

3 Results

Using all our data collected across the different methods, we observed patterns in hydrologic connectivity across our three spatial scales. At the watershed scale, we found unique patterns in soils, geomorphology, and network connectivity that provided insights to finer-scale patterns we observed. At the hydrogeomorphic feature scale, we found geomorphology influenced the dynamics of groundwater-surface water connectivity. At the hillslope scale within hydrogeomorphic features, we found unique patterns in soil structure and water table dynamics.

3.1 Watershed Scale

At the watershed scale, soil and topographic characteristics interacted to create variability in channel geomorphology. Clay-rich soils were ubiquitous throughout the watershed, with 10 of the 11 boreholes containing at least one predominantly clay horizon (Table S1). Further, predominantly clay horizons made up 32.3% of all soil described across all boreholes (Table S2). Many soil profiles also contained large amounts of sand, and the combination of these textures resulted in highly erodible soils both near the stream and across the hillslopes. Additionally, steep (20%) hillslopes paired with variably wide and low-gradient riparian corridors resulted in a mosaic of topographic conditions throughout the watershed. Slope was significantly steeper in the upper reaches of the watershed and decreased closer to the watershed outlet. Specifically, the near-channel slope was significantly steeper in the incised channel hydrogeomorphic feature than both the intact riparian zone and wetland-stream complex features ($p < 0.01$, Kruskal-Wallis Test). This aligned with our field observations of riparian corridor topographic patterns. The upper reaches of the watershed, where slope gradients were steepest and riparian corridors were narrow, were dominated by the incised channel hydrogeomorphic feature. These areas quickly transitioned to intact riparian zone features as slope decreased. Additional knickpoints resulted in larger incised channel sections occurring in the middle reaches of the watershed, and this was where the magnitude of incision between the wider riparian corridor and streambed was highest. These incised channel sections again transitioned to intact riparian zone sections, and where the riparian corridor was widest and channel slope was lowest, sediment deposition created wetland-stream complex areas closest to the outlet of our watershed. These geomorphic patterns represent the larger watershed template for the hydrologic patterns we found at the watershed and finer scales.

Across the study period, hydroclimatic variability resulted in relatively minimal network expansion and contraction. The network was fully connected in February, and drying occurred in May at two sites before completely reconnecting in August. By November, the network was dry at 6 sites. Therefore, the proportion of wet sites fluctuated from 100% to 88% throughout the year, with the driest period in November. However, ASDN length shows that the channel dynamics between the 51 observation nodes were more complex: ASDN length was highest in February at 3,700 m (100% of the potential flow network), which corresponds to the full network

extent at winter baseflow. ASDN length then decreased to 3,450 m (93%) in May before increasing slightly in August (97%) and decreasing again in November to 3,520 m (95%). However, ASDN length was lowest in May, representing 93% of the total potential flow network (Table 1). Therefore, these results suggest that the magnitude of longitudinal connectivity is temporally variable, but also strongly depends on how network connectivity is being defined (i.e., by a proportion of sites or by network length metrics). However, we acknowledge that these patterns may be biased by the above-average precipitation magnitude and disproportionately wet summer in 2021: 50% of the annual rainfall fell between June and September (NOAA National Centers for Environmental information, 2023), which aligned with the observed network expansion in August. All together, these patterns show that watershed-scale network dynamics reflected seasonal hydroclimatic variability, but that the network was relatively stable, and importantly, the magnitude and timing of variability depended on how network connectivity was defined.

Table 1. Watershed-scale results across all four seasonal surveys. Data is presented for both the site measurements (as count and percent of total) as well as the total ASDN length (as a length in m and percent of total).

Survey month	February	May	August	November
Wet sites (count)	51	49	51	45
Wet sites (%)	100	96	100	88
ASDN length (m)	3,700	3,450	3,580	3,520
ASDN length (%)	100	93	97	95
Outlet-connected site proportion (%)	100	94	100	78

Using the stream network survey data, we observed variation in network drying and channel width across hydrogeomorphic features. Of the seven sites that dried during the study period, five (71%) were sites within the incised channel hydrogeomorphic feature, compared to two intact riparian zone sites and no sites within the wetland-stream complex (Figure 2b). At the

network scale, drying occurred unevenly across the network, resulting in both contraction and disconnection. In May, both contraction and disconnection occurred equally, and in both sites where drying occurred, the drying was focused on the incised channel. In November, contraction and disconnection also occurred equally as often; however, drying occurred in four incised channel sites compared to one intact riparian zone site (Figure 2a). Additionally, only one site dried more than once, indicating hysteresis in drying within this watershed. However, we acknowledge that the irregular distribution of hydrogeomorphic features across these sites could be confounding some of these patterns.

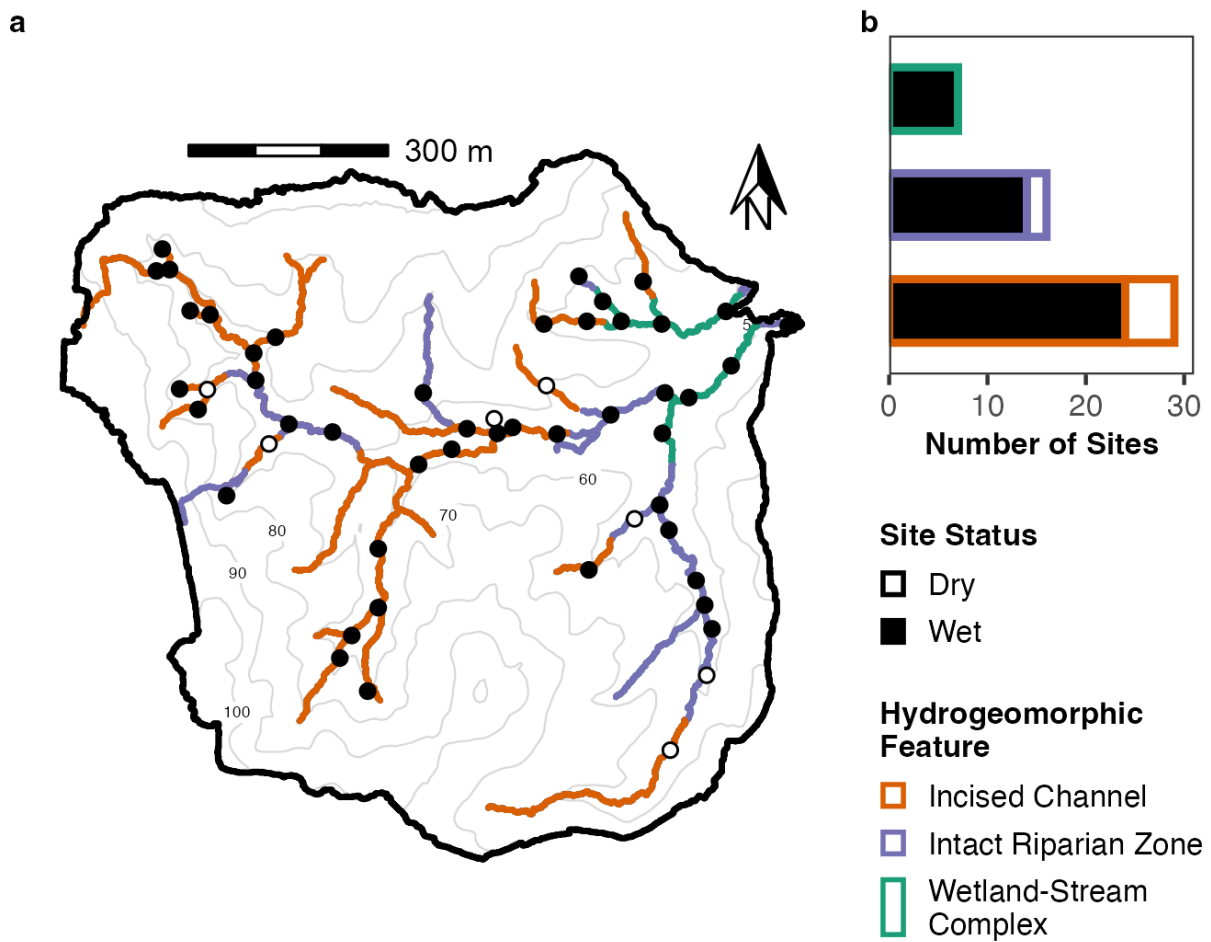


Figure 2. (a) map of the study watershed, with the stream network colored by hydrogeomorphic feature, and all survey sites marked with points ($n = 51$). Filled points represent sites that were wet at all survey timepoints, and points with no fill represent sites that dried at any point during the study. (b) is a histogram of the same 51 sites colored by hydrogeomorphic feature, indicating

the distribution of sites across the hydrogeomorphic features, as well as the proportion of wet and dry sites for each feature. Here, the incised channel had both the largest number of total sites as well as the largest number of dry sites. The intact riparian zone had the intermediate number of total sites, as well as one site that dried, and the wetland-stream complex had both the fewest total number of sites and no sites that dried.

3.2 Hydrogeomorphic Feature Scale

At the scale of hydrogeomorphic features, patterns of geomorphology between the stream and riparian zone resulted in different patterns of groundwater-surface water interactions. Water table elevation (WTE) data was used to calculate hydrologic state, where elevation gradients that were higher in the groundwater well than the in-stream well indicated gaining conditions, and an elevation gradient with the in-stream well higher than the groundwater well indicated losing conditions. We found that all hydrologic states were nearly constant throughout the study period, though the magnitude and direction of this gradient varied across hydrogeomorphic features. The incised channel was gaining across the entire study period, with an average water table slope of $+0.05$ m/m (Figure 3a,d). The intact riparian zone was losing across the entire study period, with an average water table slope of -0.05 m/m (Figure 3b,d). The wetland-stream complex was primarily at equilibrium, though there were periods of low magnitude gain and loss that resulted in an average water table slope of $+0.01$ m/m (Figure 3c,d). Additionally, we found generally gaining hydraulic gradients moving towards the stream in all transects, indicating that there was potentially a gradient pushing groundwater from the hillslope towards the stream (Table 2). This is most notable in the intact riparian zone transect, where the hydraulic gradients suggest that the floodplain is both gaining with regard to the stream and the hillslope. These patterns show a complex cascade of stream gain, loss, and equilibrium over short stream distances.

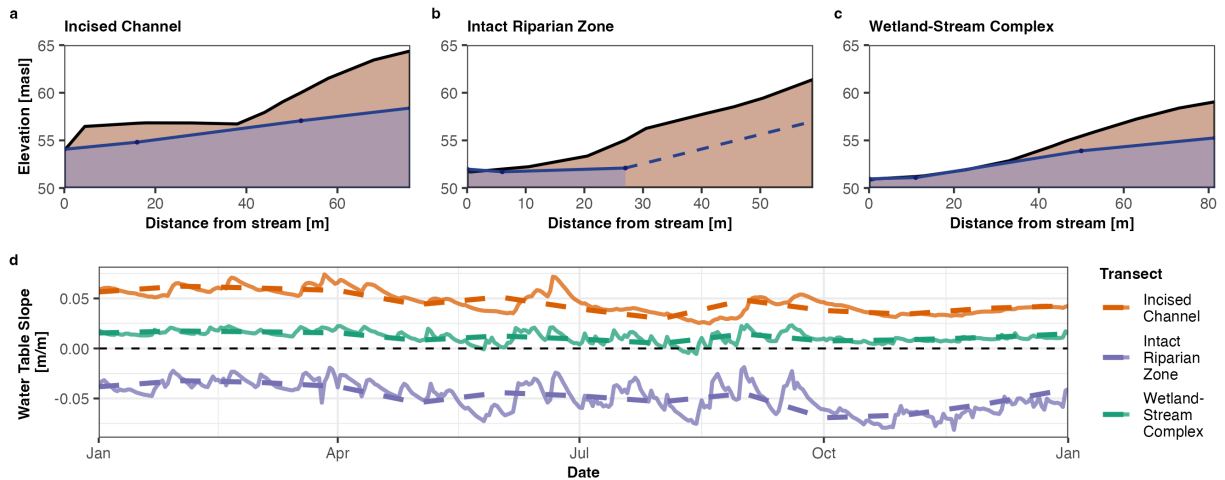


Figure 3. (a-c) cross-sections of the hillslope-riparian-stream transect, with the brown polygon corresponding to the soil surface, and the blue polygon relating to the measured annual average potentiometric surface in each of the groundwater monitoring wells. (a) indicated that the incised channel had a consistent head gradient towards the stream, indicating gaining conditions. (b) indicated that the intact riparian zone had a head gradient towards the riparian well in both directions, indicating losing conditions in the stream, but also a potential flux of groundwater from the hillslope to the riparian zone. The dashed line indicates the highest potential gradient between the lower and upper hillslope wells, as no water was ever recorded in the upper hillslope well. (c) indicated that the wetland-stream complex also had a head gradient towards the stream, suggesting gaining conditions in the channel, though at a lower gradient. (d) is both the daily (line) and monthly (dashed line) hydraulic gradient as Water Table Slope in each hydrogeomorphic feature.

Table 2. Hydraulic gradients (here, water table slope in m/m) between all wells across the hydrogeomorphic features. Data was unavailable for the Lower-Upper Hillslope Gradient in the intact riparian zone; the upper hillslope well was only saturated during precipitation events, and so a hydraulic gradient could not be calculated.

Hydrogeomorphic Feature	Stream-Riparian Gradient	Riparian-Lower Hillslope Gradient	Lower-Upper Hillslope Gradient
Incised channel	+0.05	+0.06	+0.06
Intact riparian zone	-0.05	+0.02	<i>NA</i>
Wetland-stream complex	+0.01	+0.05	+0.07

When comparing the monthly average WTE in each well to its annual average, we found distinct patterns in variability of groundwater-surface water interactions that were not completely driven by hydroclimatic variation. The wells in the incised channel transect were the most variable across space ($CV = 0.19\%$), showing high temporal variability in the groundwater wells but low variability in the stream channel (Figure 4b, Table S3). Conversely, all wells in the intact riparian zone transect were relatively stable ($CV = 0.09\%$), and variability was similar between surface water and groundwater wells (Figure 4c, Table S3). In the wetland-stream complex, there was both variability throughout space and time ($CV = 0.13\%$), but the groundwater wells were more variable than the surface water (Figure 4d, Table S3). These data show that all wells responded at different magnitudes to seasonal patterns in precipitation; all wells showed divergent responses in the incised channel regardless of water source, whereas the intact riparian zone transect showed high similarity between surface and groundwater wells, and the wetland-stream complex showed divergence between the groundwater and surface water wells, but high similarity within the groundwater wells (Figure 4).

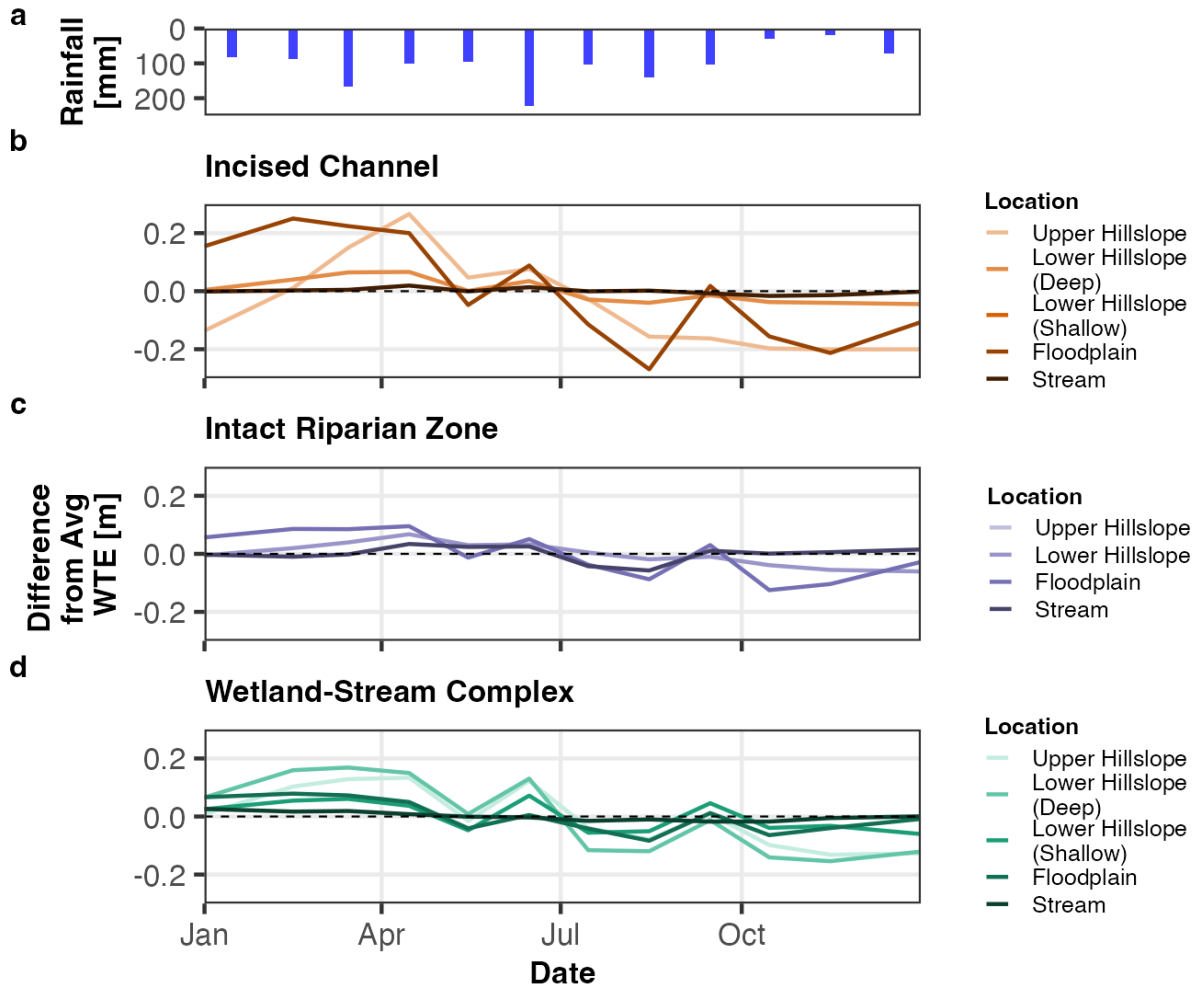


Figure 4. Difference from average WTE (calculated for each well) at monthly intervals across all three hydrogeomorphic features. (a) shows a hyetograph of monthly precipitation (mm/month) throughout the study period. (b) corresponds to the wells in the incised channel, which showed high variability throughout the study period in all groundwater wells. Conversely, the difference from average WTE in the stream channel was highly stable throughout time. (c) corresponds to the wells in the intact riparian zone, which showed the least variability throughout time. All wells were similarly variable throughout time. (d) corresponds to the wells in the wetland-stream complex, which showed moderate variability throughout time in the groundwater wells, although all wells responded similarly. The stream well was less variable throughout time.

3.3 Hillslope Scale

At the transect scale, within-hydrogeomorphic variability was observed in the soil structure and resulting hydrologic connectivity. The borehole soils data showed that while clay-textured soils were ubiquitous throughout the watershed, argillic confining horizons were not (B_{tgx} , Table S1). Argillic confining horizons were only observed in the incised channel and wetland-stream complex transects; there were no confining horizons within 4m of the surface in the intact riparian zone transect. Additionally, we found that the argillic confining horizons were not equally distributed across each hydrogeomorphic feature – they were only observed in the lower hillslope position.

The results from the ERT/TDIP transect across the wetland-stream complex hydrogeomorphic feature showed a general pattern of highly resistive material overlaying a low resistivity substrate with the exception of a part of the hillslope, where the shallow resistive material was absent and the more electrically conductive substrate reached the surface (Figure 5a). The chargeability as well as the normalized chargeability (Figure 5b,c) was generally higher within the electrically conductive substrate compared to the chargeability of the shallow electrically resistive material. We observed a conspicuous zone of high chargeability buried at approximately 1 m depth at the upper part of the hillslope (profile position 52 m to 68 m, Figure 5b). Chargeability depends on a range of physical parameters, including electrical resistivity. Slater & Lesmes (2002) found that the normalized chargeability, i.e., the chargeability divided by the electrical resistivity (Figure 5c), does not depend on the electrical resistivity and provides a substantially improved measure for clay content compared to the unnormalized chargeability. Higher normalized chargeability values were associated with a higher fraction of clay in simple sand-clay mixture lab experiments (Slater & Lesmes, 2002). From our ERT/TDIP results, together with soils data from our boreholes, we interpret that much of the hillslope was underlain by clay-rich soils. The borehole in the floodplain did not reach deep enough to confirm the clay layer indicated by the normalized chargeability results. We note that replacing the intrinsic chargeability with the integrated chargeability, or simply with the chargeability of the first time window did not affect our results.

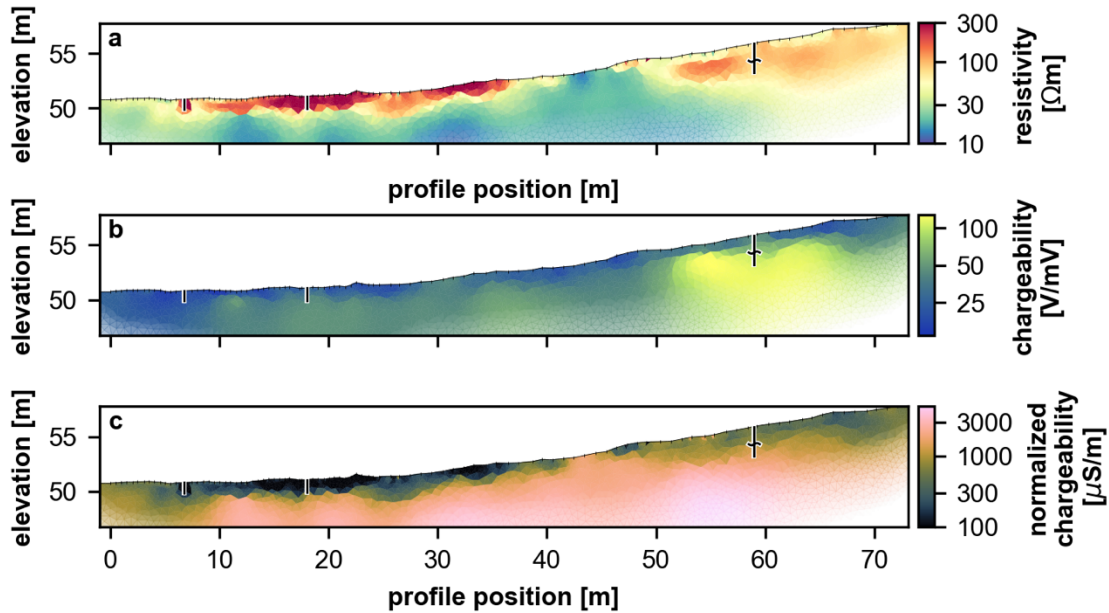


Figure 5. ERT results from the resistivity and time domain induced polarization measurements of the surveyed wetland-stream complex transect. The transect results for (a) electrical resistivity, (b) intrinsic chargeability, (c) normalized chargeability (i.e., ratio between intrinsic chargeability (b) and electrical resistivity (a)), with boreholes marked with black vertical lines indicating the elevation of the top and bottom. Additionally, locations in the boreholes where the argillic confining horizon (B_{tgx}) was located are marked with a black \sim . Together, the results suggest that there are clay-rich soils at variable depths below the surface throughout the transect.

Soil structure varied across hydrogeomorphic features, and resulted in a perched water table that also varied across hydrogeomorphic features and throughout time. A perched water table (defined by periods of inundation in the shallow nested well) was observed in both sets of nested wells. Both sets of nested wells had permanent saturation with episodic precipitation event responses in the deeper well, indicating that wells were screened into the permanent water table below the confining layer (Figure 6). Additionally, both sets of nested wells showed episodic responses to precipitation events in the shallow well (Figure 6). However, the degree of permanence of water table perching was different between hydrogeomorphic features. In the incised channel transect, water table perching was only captured in response to precipitation events, which resulted in saturation for only 15% of the period of record when compared to the permanent inundation in the corresponding deep well (Figure 6b). Conversely, the wetland-stream complex transect had permanent perching in both the shallow and deep wells, indicating

that there are two separate permanent water tables – one below the confining layer, and one perched above it (Figure 6d). All together, these results suggest that subsurface heterogeneity is influencing hydrologic connectivity throughout space, and that perched water tables vary across both space and time.

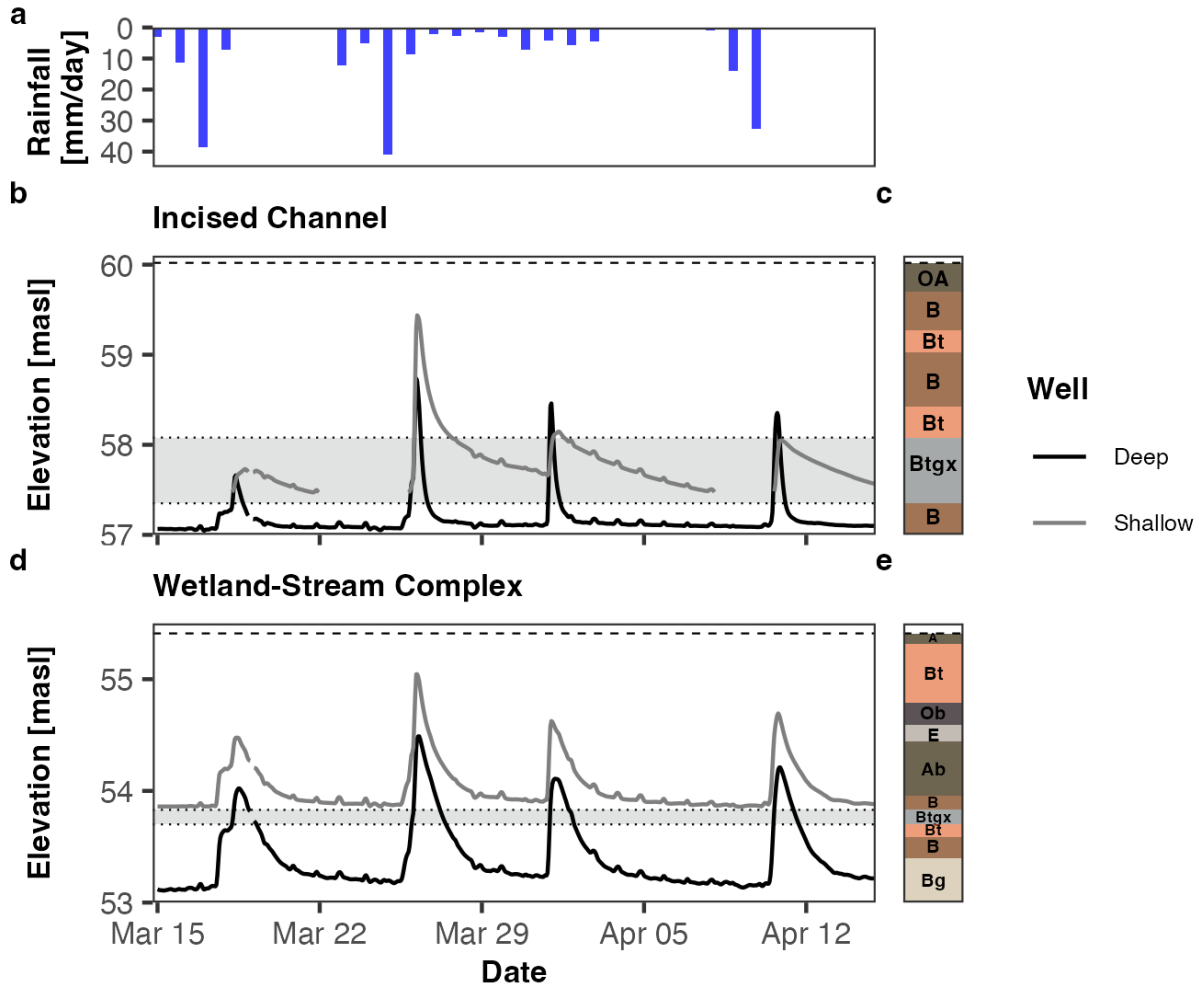


Figure 6. (a) shows a 15-day hyetograph of daily precipitation (mm/day) for the entire watershed. (b) shows 15-minute interval WTE for both nested wells in the incised channel hydrogeomorphic feature. These data suggest that there is permanent saturation below the argillic confining horizon (highlighted in grey), but only episodic perched saturation in response to storm events. (c) shows the corresponding soil profile for the nested wells in the incised channel transect, highlighting the thick argillic confining horizon (here, B_{tgx}) near the bottom of the profile. (d) shows 15-minute interval WTE for both nested wells in the wetland-stream complex hydrogeomorphic feature (where ERT/TDIP survey was conducted, shown in Figure 5

at approximately profile position 60 m). These data suggest that there is also permanent saturation below the argillic confining horizon (highlighted in grey), but additionally, permanent saturation above it. Therefore, these results suggest that there are two permanent water tables in this hydrogeomorphic feature. (e) shows the corresponding soil profile for the nested wells in the wetland-stream complex, highlighting the thin $B_{t_{gx}}$ horizon near the middle of the profile.

4 Discussion

4.1 Hydrogeomorphic features can be used as a template for river corridor structure

Our understanding of hydrologic processes is limited by the spatial and temporal scale of our measurements; hydrogeomorphic features provide an intermediate scale that can be used to better understand hydrologic connectivity and storage along the river corridor. All watersheds have some degree of heterogeneity regardless of size or location (McDonnell et al., 2007; Wainwright et al., 2022), and variability in structural landscape characteristics results in heterogeneity of hydrologic connectivity across scales ranging from soil pedons to large watersheds (McDonnell et al., 2007; Rinderer et al., 2018; Sivapalan, 2006). Feedbacks and interactions within and across scales result in emergent properties (i.e., connectivity), and therefore watershed responses are driven by processes occurring in and across hierarchical scales (McDonnell et al., 2007; Poff, 1997; Wohl et al. 2019). However, it is difficult to measure and predict heterogeneity across scales without a clear understanding of the physical processes that have created modern structural connectivity (Sivapalan, 2006; Troch et al., 2009). To aid this, many studies have suggested organizing watersheds into functional groups (McDonnell et al., 2007), geomorphic units (Schumm, 1977), and process domains (Montgomery, 1999). However, many of these characterizations have focused on larger spatial and temporal scales and do not account for hierarchical or nested scales (Wymore et al., 2023). We suggest that discretizing river corridors into smaller hydrogeomorphic features based on observable structural differences provides the opportunity to characterize the heterogeneities and processes occurring at subordinate scales. Therefore, with a better understanding of structural connectivity at finer scales, emergent properties of functional connectivity can be quantified in the larger watershed.

Here, we provide a perceptual model (e.g., Wagener et al., 2021, McMillan et al., 2023) of the patterns of structural connectivity and its implications for storage and functional

connectivity across hydrogeomorphic features in our watershed. Foundationally, all hydrologic processes within this watershed are the result of and contributors to landscape evolution across temporal scales (van der Meij et al., 2018). At the largest timescales, climate and geology interact to determine the physiographic template of the region (Miller & Robinson, 1995; Montgomery, 1999). The primary drivers of landscape evolution interact throughout time to influence topography (Montgomery, 1999; Schumm, 1977). At shorter timescales, natural disturbances (e.g., debris flows, Montgomery & Dietrich, 1994) or anthropogenic modifications (e.g., flow control structures, Wohl, 2006) further interact with the physiographic and topographic templates to determine watershed-scale patterns (van der Meij et al., 2018). Together, feedbacks between landscape drivers and changes influence the modern hydrologic, pedologic, and geomorphic conditions in a watershed, which result in patterns of structural connectivity (Larsen et al., 2012; van der Meij et al., 2018; Rinderer et al., 2018). In our study watershed, these conditions result in three distinct hydrogeomorphic patterns occurring in a predictable cascade: erosional headwaters that flow into transport-dominated streams, which then flow into depositional wetlands (*sensu* Schumm, 1977; Montgomery, 1999; Jaeger et al., 2017). In our watershed, these hydrogeomorphic features have resulted in distinct drivers of structural connectivity at the shortest timescales; we define these drivers here as stream incision, channel cross-sectional area, and soil heterogeneity (Figure 7).

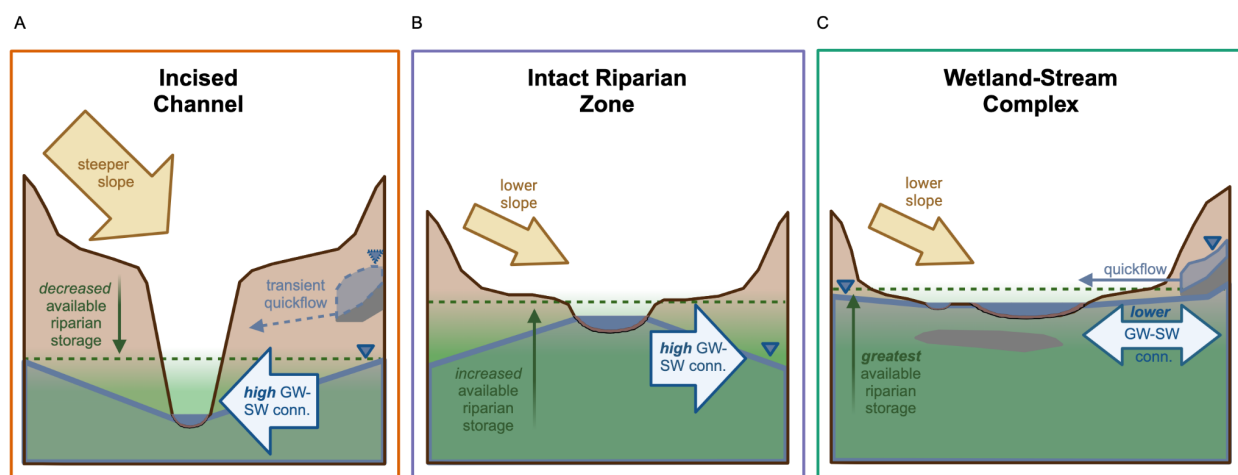


Figure 7. Our perceptual model for the primary structural and functional features of the river corridor across our hydrogeomorphic features. (a) shows the patterns in the incised channel, where introduced incision results in decreased available riparian storage, and high unidirectional groundwater-surface water connectivity toward the stream. (b) shows the patterns in the intact

riparian zone, where increased available riparian storage and smaller channel area results in high unidirectional groundwater-surface water connectivity away from the stream. (c) shows the patterns in the wetland-stream complex, where the greatest available riparian storage and additional floodplain wetlands result in decreased, bidirectional groundwater-surface water connectivity.

Our results suggest that hydrogeomorphic features influence available riparian storage through spatial changes in valley slope, stream incision, and channel cross-sectional area (Figure 7). Changes in storage across space (e.g., channel incision, soil structure) result in differences in hydrologic state and subsequent groundwater-surface water connectivity between hydrogeomorphic features, which directly translates to either groundwater discharges to the stream (in gaining conditions) or groundwater recharge from surface water (in losing conditions) (Figure 7). Further, spatial and temporal patterns in hydrologic connectivity can also be influenced by spatiotemporal heterogeneity in the activation of perched flowpaths. All together, these interactions of storage and connectivity across hydrogeomorphic features highlight potential sources of variability in processes along river corridors.

Our perceptual model of hydrologic connectivity across hydrogeomorphic features allows us to integrate all compartments of the river corridor. While other landscapes may differ in physiographic templates, land use histories, and subsequent structural connectivity, the concept of physically-based hydrogeomorphic features presented here may be applicable to other low-gradient, highly erodible landscapes. Erosive processes like incision and gully formation have been well documented, both across low-gradient systems in the southeastern USA and across the globe (Galang et al., 2007; Poesen et al., 2003). Cascades of sediment production, transport, and deposition occur in predictable patterns across river systems due to erosion and deposition processes that are driven by topographic gradients (Montgomery, 1999; Schumm, 1977). Gully erosion, stream incision, and other erosive processes are common in the Coastal Plain and Piedmont physiographic regions due to their highly erodible soils and land-use histories, but many other low-gradient systems are also prone to gully formation due to anthropogenic influence (Chen et al., 2020; Trimble, 2021).

Gully erosion and stream incision are both legacy effects driven by land-use changes (Galang et al., 2007; Maloney et al., 2008; Willgoose et al., 1991), which can also increase groundwater-surface water connectivity, lower water tables, and increase flashiness and aridification (Chen et al., 2020; Valentin et al., 2005; Vanmaercke et al., 2021). However, to understand how legacy effects like erosion and incision can both influence the distribution of hydrogeomorphic features and result in long-term hydrologic legacy effects, it is important to first characterize how watershed hydrogeomorphic features can influence watershed structural and functional hydrologic connectivity. Further, this is the first study to document clear differences in functional connectivity across these hydrogeomorphic features, rather than just in regions of gully formation (Chen et al., 2020). Therefore, we expect that these physically-based hydrogeomorphic features could be leveraged to better understand finer-scale patterns of surface water-groundwater interactions across watersheds and scales in low-gradient systems with land-use legacies.

4.2 Hydrologic state demonstrates the relationships between structural and functional connectivity across hydrogeomorphic features

Across hydrogeomorphic features, differences in structural connectivity defined by physical features result in distinct patterns of hydrologic connectivity. Differences in subsurface architecture, topography, and even riparian vegetation have resulted in physical templates that influence the functional hydrologic connectivity of these regions. Incision-induced hydraulic head gradients and heterogeneities in water storage and sources can result in unique patterns of surface water-groundwater interactions and streamflow generation. Therefore, we expect that hydrologic state and water table variability reflect the relationships between surface and subsurface storage across hydrogeomorphic features.

4.2.1 Incised Channel Hydrogeomorphic Feature

Structurally, the incised channel hydrogeomorphic feature represents an erosion-dominated zone with little available riparian storage. In our study watershed, sections of the river corridor in the incised channel zone are farthest upstream in the network (Figure 2), and often initiate at obvious channel heads that formed at knickpoints in clay soil horizons or vegetative structures. These areas of incised channel features occur in the areas of steepest watershed

slope, which aligns with observations from other studies (e.g., Menéndez-Duarte et al., 2007; Schumm, 1977). Incision results in a decrease in the available storage of the riparian zone, as water table lowering has decreased the soil storage that can be accessed by the stream (Figure 7). Further, the stream has become disconnected from the riparian floodplain, meaning that there is no capacity for event-driven bidirectional flow (e.g., Squillace, 1996; Zimmer & McGlynn, 2018). However, channel incision also results in an increase in total channel cross-sectional area, which increases the stream's water transport capacity (e.g., Simon & Rinaldi, 2006). Additionally, the soils in this hydrogeomorphic feature are the least organic with high clay proportions, which decreases the ability for water to move through the soil and increases preferential flow. Altogether, streams in these incised channel zones represent both the feedbacks from and causes of increased erosion due to anthropogenic impacts.

Functionally, these structural characteristics interact to create a hydrologically stable channel that was gaining across the duration of the study, meaning that there was consistent groundwater discharge into the stream channel from the nearby riparian zone (Figure 7). The observed head gradient is likely a result of the elevation gradient that stream incision introduced (Chen et al., 2020). Further, the hydrologic state results align with our hydrogeomorphic perceptual model – the decreased riparian storage will result in higher groundwater discharges to the stream, and the increased channel cross-sectional area will result in export of that water downstream rather than bidirectional flow back into the riparian groundwater (e.g., Hester et al., 2020; Hucks Sawyer et al., 2009; Zimmer & McGlynn, 2018). Our finding that surface water and groundwater responded to seasonal precipitation patterns dissimilarly agrees with our perceptual model; the hydrologic gradient introduced by the stream incision and constant gaining conditions results in highly temporally stable streamflow. Further, the dissimilarity between the surface water and the groundwater wells suggests a decoupling between the riparian corridor and the hillslope. All together, these results indicate that in terms of functional connectivity, streams in incised channel features are highly connected to the groundwater through unidirectional hydraulic gradients that generate stable streamflow.

Our results suggest that the structure of the incised channel increases the duration and magnitude but decreases the variability of hydrologic connectivity. The unidirectional hydraulic gradient introduced by stream incision resulted in short-term increases in the connected channel

network, as the constant groundwater discharge creates more stable flow in these sections of the river corridor, which contrasts with previous studies (Chen et al., 2020). However, at longer timescales, this likely results in lowered capacity for network connectivity by decreasing water availability, which has been suggested by other studies (Chen et al., 2020; Valentin et al., 2005). All together, these results show the effects of decreasing available riparian storage, which is a positive feedback that further exacerbates decreased water availability.

These patterns in riparian water availability across timescales then have long-term implications for ecosystem functions. Decreases in available riparian storage result in lowered water tables and increased aridification, which can have negative effects on riparian vegetation as the water table recedes below rooting depths and reduces water available for transpiration (Loheide & Booth, 2011; Valentin et al., 2005; Vanmaercke et al., 2021). Further, the separation from the stream to the riparian floodplain also reduces the opportunity for groundwater recharge, as during stormflows the stream is not able to expand laterally into the floodplain and recharge riparian groundwater when compared to non-incised channels (Jung et al., 2004; Winter, 1995; Zimmer & McGlynn, 2018). All together, these results show that complex feedbacks between channel incision, hydrogeomorphology, and resulting ecosystem function will continue to have legacy effects on these river corridors and watersheds.

4.2.2 Intact Riparian Zone Hydrogeomorphic Feature

Structurally, the intact riparian zone represents a transport-dominated feature with high available riparian storage. Streams in the intact riparian zone hydrogeomorphic feature were defined as having clear bed-and-bank structure and access to an obvious riparian zone (delineated by riparian vegetation such as Florida anise, *Illicium floridanum*) that was incised < 0.5 m. In our study watershed, these sections of the river corridor tend to occur in the middle portions of the network. Intact riparian zones are always downstream of incised channels, where the valley begins to widen, slope decreases, and channels shift from erosion-dominated to transport-dominated (Schumm, 1977). Unlike the incised channel feature, streams in the intact riparian zone have access to their adjacent floodplains during high flows, which results in high available riparian storage as well as the opportunity for bidirectional event-driven flow and groundwater recharge (Jung et al., 2004; Zimmer & McGlynn, 2018). Intact riparian zone

streams have the lowest cross-sectional channel area paired with decreased slope, resulting in reduced ability for the stream to route water through the network. This likely translates to an increased residence time of water in the channel and this section of the river corridor. Further, intact riparian zones are predominantly composed of sandy substrate, and the soils in these areas are predominantly sandy clays as a result, which has a higher permeability than upstream incised channel soils.

Functionally, across the intact riparian zone we observe a hydraulic gradient from the stream to the adjacent riparian zone. This gradient suggests the stream was consistently and significantly losing during the study period, resulting in unidirectional surface water recharge to the riparian groundwater. Unlike the incised channel, we expect that the losing conditions were a direct result of the same volume of water discharging into a region of increased available riparian storage, which aligns with our conceptualization of this hydrogeomorphic feature (Figure 7). This conceptualization also agrees with our findings of high similarity in water table response across all wells and greater stream variability, where consistent losing conditions results in riparian groundwater response mirroring stream conditions, and those stream conditions varying throughout time. Our network length results also agree with this conceptualization, as surface waters in the intact riparian zone are losing water to the subsurface and therefore will have more variability when upstream flows decrease. All together, these results indicate that in terms of functional connectivity, the intact riparian zone is highly responsive to upstream flows as well as a region of groundwater recharge.

These patterns of structural and functional connectivity highlight the dynamic and transitional nature of the intact riparian zone hydrogeomorphic feature. The combination of upstream flows and local interactions between the stream and riparian zone result in highly hydrologically connected river corridors. Riparian zones play an important role in regulating the physical, chemical, and biological functions of aquatic ecosystems, and represent a dynamic interface between aquatic and terrestrial zones (Junk et al., 1989). Hydrologically, these sections of the river corridor are key zones of groundwater recharge, even at baseflow (Jung et al., 2004; Winter, 1995) and can potentially serve as disconnectivity points at lower flows (Godsey & Kirchner, 2014; Larned et al., 2011). Additionally, the high hydrologic connectivity we observed can result in bidirectional flows from storm event to seasonal timescales (e.g., Hucks Sawyer et

al., 2009; Zimmer & McGlynn, 2018), which shows the relative importance and tight coupling of these river corridors with their riparian zones. Biogeochemically, riparian zones are key sites of nutrient flux and transformation (Gu et al., 2012; McClain et al., 2003; McGlynn & McDonnell, 2003). Ecologically, riparian zones provide high water availability for vegetation due to shallow water tables (Burt et al., 2002; Swanson et al., 1982), and can serve as refugia for organisms during stormflows and increase habitat complexity (Junk et al., 1989; Tockner et al., 2000). Therefore, our results highlight the role these highly connected river corridors play in regulating local ecosystem functions as well as upstream hydrologic conditions.

4.2.3 Wetland-Stream Complex Hydrogeomorphic Feature

Structurally, the wetland-stream complex represents a deposition-dominated zone with high available riparian storage. Wetland-stream complexes were defined here as river corridors where the low-gradient stream anastomosed between riparian wetlands and were highly depositional areas for sediment and organic matter (Schumm, 1977). In our study watershed, the wetland-stream complex is the most downstream region of the network and occurs in wide U-shaped valleys. Like streams in the intact riparian zone, wetland-stream complexes have full access to their riparian floodplains, and in addition, have access to isolated surface-water wetlands during high flows. This access results in both high available riparian storage in both the surface and subsurface, and the potential for both lateral surface water flows and bidirectional flows during events (*sensu* Ward, 1989; Zimmer & McGlynn, 2018). Additionally, because of the structure of the river corridor, streams in the wetland-stream complex region have moderately high cross-sectional channel areas. Channels in this hydrogeomorphic feature have highly organic sediments, as well as highly organic riparian soils, which results in both greater hyporheic flows and subsurface permeability. Altogether, the wetland-stream complex was a dynamic downvalley system with low-gradients and high riparian available storage.

Functionally, these structural features create sections of the river corridor that are variable in flow and controlled by both upstream and local conditions. The wetland-stream complex was at an equilibrium throughout the period of record – there was primarily a slightly gaining hydraulic gradient, but the wetland-stream complex was also the only feature that fluctuated between hydrologic states at any point (i.e., from gaining most days to losing others,

Figure 3). Therefore, this hydrogeomorphic feature is the only one with measured bidirectional flows, which is a result of both upstream and local conditions. Given that this feature has high available riparian storage in surface water and groundwater, the hydrologic state of the wetland-stream complex is controlled by the flow it receives from upstream in addition to local groundwater contributions.

Further, the wetland-stream complex had the greatest available riparian storage. The low incision results in high available storage of the riparian zones similarly to the intact riparian zone, but the increased channel footprint results in higher storage capacity of the channel similarly to the incised channel (Figure 7). This aligns with our findings that there was high similarity among groundwater wells, but divergence between groundwater and surface water – suggesting a decoupling of the stream from the river corridor, given that surface water is influenced by upstream conditions. Therefore, our results show that the wetland-stream complex modulates both upstream surface flows and local subsurface flows to maintain a stable channel, which aligns with findings in other wetland-dominated areas (e.g., Bullock & Acreman, 2003; McLaughlin et al., 2014; Wegener et al., 2017). This further aligns with our network length results, where no sites in the wetland-stream complex dried. All together, these results indicate that wetland-stream complexes are dynamic zones that modulate bidirectional fluxes between surface and groundwater sources.

These results highlight the role wetland-stream complexes play on integrating upstream and local signals. Given that this hydrogeomorphic feature is located at the most downstream portion of the study watershed, sections of the river corridor in this zone are integrating water, sediment, and landscape processes across space and time. Wetlands generally are key sites of connectivity between terrestrial riparian zones and aquatic ecosystems, as their stable flows provide refugia for organisms and increased water availability for hydrophytic vegetation (Leibowitz et al., 2018; Leigh et al., 2010). Stable flows and high organic content in the sediments make these sections of the river corridor hotspots of nutrient processing, especially denitrification and other anaerobic processes (Cheng & Basu, 2017; McClain et al., 2003). Further, bidirectional flows and lateral exchange flows also allow for increased groundwater recharge on shorter storm-event timescales (Jung et al., 2004; Ward, 1989). Therefore, the patterns we observed in hydrologic connectivity in this hydrogeomorphic feature highlight the

role wetlands play in modulating upstream and local conditions to serve as key regulators of ecosystem function.

4.3 Perched flowpath activation demonstrates spatial and temporal heterogeneity within hydrogeomorphic features

Within hydrogeomorphic features, fine-scale heterogeneity in structural connectivity drives the location and magnitude of perched flowpaths. Perched flowpaths are driven by confining layers and soil horizons with contrasting hydraulic conductivities (Baird & Low, 2022; Weyman, 1973). Activation of these perched flowpaths represents a form of quickflow (i.e., shallow subsurface flow that is routed to the stream rapidly in response to precipitation events through matrix or preferential flow, *sensu* Carey & Woo, 2001; Scaife et al., 2020) between surface water and groundwater, and can have a variety of impacts on hydrologic connectivity across timescales. At short timescales, this quickflow can result in flashier streamflow responses to storm events, and at longer timescales, can result in decreased groundwater recharge as infiltration is routed to surface water rather than groundwater (McDaniel et al., 2008; Niswonger & Fogg, 2008; Zimmer & McGlynn, 2017). In our study, perched flow was observed to only occur in the lower hillslope position, where confining clay horizons were within 4 m of the soil surface. However, the ERT/TDIP survey demonstrated that a high normalized chargeability layer (Figure 5c), which we interpret to be a confining clay layer, was heterogeneous in depth across space, occurring at variable depths within the subsurface. Therefore, we expect that perched flow is likely distributed patchily in this watershed and does not contribute equally to streamflow in all hydrogeomorphic features nor even within any given hydrogeomorphic feature. This patchiness may affect whether perched flowpaths affect groundwater recharge and quickflow responses.

Additionally, the timing of perched flowpath activation differed across hydrogeomorphic features, which could result in variability in streamflow generation processes. As discussed, perched flow can represent a distinct source of streamflow generation, as well as variability in that source throughout time (Niswonger & Fogg, 2008; Zimmer & McGlynn, 2017). Perched flow was ephemeral in the incised channel hydrogeomorphic feature given that it was only observed 15% of the study period, and only in response to storm events and likely higher

antecedent soil moisture. This likely means that in the incised channel hydrogeomorphic feature, perched flowpath activation represents quickflow, and contributions to streamflow are limited to event runoff. However, perched flow was perennial in the wetland-stream complex, which could mean that streamflow is potentially a mixture of shallow and deep groundwater depending on the distribution of confining clay horizons in the riparian zone (similarly to the findings in Zimmer & McGlynn, 2018). Therefore, the timing and magnitude of perched flow contributions to streamflow likely differ through space and time.

Together, these results suggest that fine-scale heterogeneity in subsurface structure has implications for larger watershed processes. Emergent watershed properties have been well documented and are ubiquitous across systems regardless of watershed size (i.e., Musolff et al., 2017; Shogren et al., 2019; Jencso et al., 2009; McDonnell et al., 2007) and represent the feedbacks of processes occurring across subsequent smaller scales (Gentine et al., 2012; Laudon & Sponseller, 2018; McDonnell et al., 2007). Previous studies have shown that heterogeneity at finer scales (e.g., TTDs in individual hillslopes, Harman, 2015; soil hydraulic conductivity properties, Weyman, 1973) drive the patterns of runoff generation and hydrologic processes at coarser scales (e.g., water age distributions at watershed outlets, Harman, 2015; McGuire et al., 2005). However, it is still difficult to predict watershed-scale patterns using finer-scale heterogeneities given the existing gap between patterns and process (Jencso et al., 2009). Therefore, we expect that incorporating hillslope and hydrogeomorphic feature processes will improve modeling of the patterns of runoff generation at the watershed scale. Here, we have made an initial attempt to describe potential heterogeneities that are likely important, despite not capturing all processes at all scales.

Further, we acknowledge that our understanding of streamflow generation in these areas is limited by our methods: our monitoring wells measured hydraulic head gradients and were unable to quantify flux, so we are unable to quantify how much of the observed perched flow is routed to streamflow. Additionally, our wells were only able to measure saturation, while some (albeit, small) portion of quickflow can also be unsaturated interflow through the soil matrix, which we are unable to account for. Despite these limitations, however, we anticipate that the spatial and temporal patterns of perched flowpath activation reveal the influence of subsurface heterogeneity on hillslope-scale hydrologic connectivity.

4.4 Implications

Altogether, we suggest that hydrologic connectivity can be defined operationally at the hydrogeomorphic feature scale, as this scale allows us to better quantify processes across the river corridor that control watershed-scale responses. It has been well-documented that characterizing watershed processes across spatial scales is difficult due to the nestedness of process and emergent properties; that is, the scale of study affects the results (e.g., McDonnell et al., 2007). Additionally, the intermediate scales are often the hardest to define. Plot-scale hillslope hydrology and reach-scale hyporheic studies have helped us better understand fine-scale heterogeneities and processes. Conversely, watershed-scale hydrology and continental-scale comparison studies have helped us develop overarching principles for the drivers of streamflow generation across regions (e.g., Wymore et al., 2023). However, multiple definitions of the intermediate scale (e.g., process domains, geomorphic units, or river corridors (Montgomery, 1999; Schumm, 1977; Harvey & Gooseff, 2015) have skewed our understanding of subsequent processes to specific locations and regions. Further, these definitions are still immensely spatially variable, ranging from multiple stream reaches to entire basins. Therefore, we propose that using hydrogeomorphic features will further enable investigations of the river corridor that integrate both upstream influences with adjacent lateral hydrological processes.

5 Conclusions

We measured hydrologic connectivity across dimensions and scales to characterize potential drivers of streamflow generation in a headwater system in the Coastal Plain physiographic province. We used hydrogeomorphic feature as an intermediate spatial scale that could be used to quantify hydrologic processes across the river corridor. In Coastal Plain settings, headwater systems often have cascades of incised channels, intact riparian zones, and wetland-stream complexes occurring across small (< 200 m) spatial scales. Our study found distinct patterns of hydrologic connectivity across these hydrogeomorphic features, in addition to distributed patches of perched flowpaths. All together, these results show the importance of considering hydrologic fluxes across both dimensions and scales and provide an initial characterization of streamflow generation in an understudied low-gradient region. The Coastal Plain is a nationally expansive region, and its highly weathered and deep soils paired with humid climate and land-use legacies

provide an opportunity to study potentially unique drivers of hydrologic fluxes at small scales. Given the results of this study, we suggest that further work should be done to understand the role of preferential flow and transient, perched flowpaths on streamflow generation, as the patchy distribution of argillic confining horizons within watersheds is likely a potential factor in the timing and magnitude of hydrologic fluxes in these watersheds. While these results are limited by the scope of one watershed, we believe that both hydrogeomorphic features as a scale of study and potential drivers of streamflow identified here can be used further, both in Coastal Plain watersheds and headwater systems across diverse physiographic provinces.

Acknowledgments

The authors received support from the AIMS Project (funded by the National Science Foundation, Award Number 2019603); the FLOODPULSE Project (funded by the U.S. Department of Energy, Office of Science, Office of Biological and Environmental Research, Award Number DE-SC0023469), and the Alabama Water Institute. The authors would like to thank Dr. Corianne Tatariw, Matthew Shockey, Kevin Shaw, Timothy Bushman, Vanessa Marshall, Stella Wilson, Dr. Jacob Dybiec, and many other friends and colleagues for their invaluable help with instrument installation and extensive fieldwork. We would also like to thank Dr. Adam Price, Dr. Ashleigh Kirker, Dr. Carla Atkinson, and Dr. Jon Benstead for their helpful feedback on ideas and early versions of the manuscript. We also thank the editor and anonymous reviewers for their time and effort in providing valuable feedback. The authors declare no conflicts of interest relevant to this study.

Open Research

Hydrologic sensor data is available on ESS-DIVE. Electrical Resistivity Tomography data and scripts is available here: [10.5281/zenodo.12766587](https://doi.org/10.5281/zenodo.12766587) All other data and programs used for this study have been cited above, and found publicly available at the locations listed in the references.

References

- Aho, K., Derryberry, D., Godsey, S. E., Ramos, R., Warix, S. R., & Zipper, S. (2023). Communication Distance and Bayesian Inference in Non-Perennial Streams. *Water Resources Research*, 59(11), e2023WR034513. <https://doi.org/10.1029/2023WR034513>
- Alabama Cooperative Extension System. (2018). *Alabama Soils: Coastal Plain*. Retrieved September 27, 2023, from <https://www.aces.edu/blog/topics/healthy-soils/alabama-soils-coastal-plain/>
- Alexander, R. B., Boyer, E. W., Smith, R. A., Schwarz, G. E., & Moore, R. B. (2007). The Role of Headwater Streams in Downstream Water Quality¹. *JAWRA Journal of the American Water Resources Association*, 43(1), 41–59. <https://doi.org/10.1111/j.1752-1688.2007.00005.x>
- Allen, G. H., Pavelsky, T. M., Barefoot, E. A., Lamb, M. P., Butman, D., Tashie, A., & Gleason, C. J. (2018). Similarity of stream width distributions across headwater systems. *Nature Communications*, 9(1), 610. <https://doi.org/10.1038/s41467-018-02991-w>
- Neilson, M. (2007). *East Gulf Coastal Plain Physiographic Section*. Encyclopedia of Alabama. Retrieved January 19, 2022, from <http://encyclopediaofalabama.org/article/h-1256>
- Baird, A. J., & Low, R. G. (2022). The water table: Its conceptual basis, its measurement and its usefulness as a hydrological variable. *Hydrological Processes*, 36(6), e14622. <https://doi.org/10.1002/hyp.14622>
- Botter, G., & Durighetto, N. (2020). The Stream Length Duration Curve: A Tool for Characterizing the Time Variability of the Flowing Stream Length. *Water Resources Research*, 56(8), e2020WR027282. <https://doi.org/10.1029/2020WR027282>
- Bracken, L. J., Wainwright, J., Ali, G.A., Tetzlaff, D., Smith, M.W., Reaney, S.M., & Roy, A.G. (2013). Concepts of hydrological connectivity: Research approaches, pathways and future agendas. *Earth-Science Reviews*, 119(1), 17-34. <https://doi.org/10.1016/j.earscirev.2013.02.001>
- Bullock, A., & Acreman, M. (2003). The role of wetlands in the hydrological cycle. *Hydrology and Earth System Sciences*, 7(3), 358–389. <https://doi.org/10.5194/hess-7-358-2003>
- Burt, T. P., & McDonnell, J. J. (2015). Whither field hydrology? The need for discovery science and outrageous hydrological hypotheses. *Water Resources Research*, 51(8), 5919–5928. <https://doi.org/10.1002/2014WR016839>

- Burt, T. P., Pinay, G., Matheson, F. E., Haycock, N. E., Butturini, A., Clement, J. C., et al. (2002). Water table fluctuations in the riparian zone: comparative results from a pan-European experiment. *Journal of Hydrology*, 265(1), 129–148.
[https://doi.org/10.1016/S0022-1694\(02\)00102-6](https://doi.org/10.1016/S0022-1694(02)00102-6)
- Cardenas, M. B., Wilson, J. L., & Zlotnik, V. A. (2004). Impact of heterogeneity, bed forms, and stream curvature on subchannel hyporheic exchange. *Water Resources Research*, 40(8).
<https://doi.org/10.1029/2004WR003008>
- Carey, S. K., & Woo, M. (2001). Slope runoff processes and flow generation in a subarctic, subalpine catchment. *Journal of Hydrology*, 253(1), 110–129.
[https://doi.org/10.1016/S0022-1694\(01\)00478-4](https://doi.org/10.1016/S0022-1694(01)00478-4)
- Chen, X., Kumar, M., Richter, D. deB, & Mau, Y. (2020). Impact of gully incision on hillslope hydrology. *Hydrological Processes*, 34(19), 3848–3866.
<https://doi.org/10.1002/hyp.13845>
- Cheng, F. Y., & Basu, N. B. (2017). Biogeochemical hotspots: Role of small water bodies in landscape nutrient processing. *Water Resources Research*, 53(6), 5038–5056.
<https://doi.org/10.1002/2016WR020102>
- Costigan, K. H., Jaeger, K. L., Goss, C. W., Fritz, K. M., & Goebel, P. C. (2016). Understanding controls on flow permanence in intermittent rivers to aid ecological research: integrating meteorology, geology and land cover. *Ecohydrology*, 9(7), 1141–1153.
<https://doi.org/10.1002/eco.1712>
- Covino, T. (2017). Hydrologic connectivity as a framework for understanding biogeochemical flux through watersheds and along fluvial networks. *Geomorphology*, 277, 133–144.
<https://doi.org/10.1016/j.geomorph.2016.09.030>
- Davis, M. E. (1988). *Stratigraphic and hydrogeologic framework of the Alabama Coastal Plain*, (Water-Resources Investigations Report No. 87–4112). U.S. Geological Survey.
Retrieved from <https://pubs.usgs.gov/publication/wri874112>
- Downing, J. A., Cole, J. J., Duarte, C. M., Middelburg, J. J., Melack, J. M., Prairie, Y. T., et al. (2012). Global abundance and size distribution of streams and rivers. *Inland Waters*, 2(4), 229–236. <https://doi.org/10.5268/IW-2.4.502>
- Doyle, M., & Ensign, S. (2009). Alternative Reference Frames in River System Science. *BioScience*, 59(6), 499–510. <https://doi.org/10.1525/bio.2009.59.6.8>

- Dunne, T., & Black, R. D. (1970). An Experimental Investigation of Runoff Production in Permeable Soils. *Water Resources Research*, 6(2), 478–490.
<https://doi.org/10.1029/WR006i002p00478>
- Epps, T. H., Hitchcock, D. R., Jayakaran, A. D., Loflin, D. R., Williams, T. M., & Amatya, D. M. (2013). Characterization of Storm Flow Dynamics of Headwater Streams in the South Carolina Lower Coastal Plain¹. *JAWRA Journal of the American Water Resources Association*, 49(1), 76–89. <https://doi.org/10.1111/jawr.12000>
- Foster, D., Swanson, F., Aber, J., Burke, I., Brokaw, N., Tilman, D., & Knapp, A. (2003). The Importance of Land-Use Legacies to Ecology and Conservation. *BioScience*, 53(1), 77–88. [https://doi.org/10.1641/0006-3568\(2003\)053\[0077:TIOLUL\]2.0.CO;2](https://doi.org/10.1641/0006-3568(2003)053[0077:TIOLUL]2.0.CO;2)
- Galang, M. A., Markewitz, D., Morris, L. A., & Bussell, P. (2007). Land use change and gully erosion in the Piedmont region of South Carolina. *Journal of Soil and Water Conservation*, 62(3), 122–129.
- Gentine, P., Troy, T. J., Lintner, B. R., & Findell, K. L. (2012). Scaling in Surface Hydrology: Progress and Challenges. *Journal of Contemporary Water Research & Education*, 147(1), 28–40. <https://doi.org/10.1111/j.1936-704X.2012.03105.x>
- Godsey, S. E., & Kirchner, J. W. (2014). Dynamic, discontinuous stream networks: hydrologically driven variations in active drainage density, flowing channels and stream order. *Hydrological Processes*, 28(23), 5791–5803. <https://doi.org/10.1002/hyp.10310>
- Gomi, T., Sidle, R. C., & Richardson, J. S. (2002). Understanding Processes and Downstream Linkages of Headwater Systems: Headwaters differ from downstream reaches by their close coupling to hillslope processes, more temporal and spatial variation, and their need for different means of protection from land use. *BioScience*, 52(10), 905–916.
[https://doi.org/10.1641/0006-3568\(2002\)052\[0905:UPADLO\]2.0.CO;2](https://doi.org/10.1641/0006-3568(2002)052[0905:UPADLO]2.0.CO;2)
- Grabowski, R. C., & Gurnell, A. M. (2016). Hydrogeomorphology—Ecology Interactions in River Systems. *River Research and Applications*, 32(2), 139–141.
<https://doi.org/10.1002/rra.2974>
- Gu, C., Anderson, W., & Maggi, F. (2012). Riparian biogeochemical hot moments induced by stream fluctuations. *Water Resources Research*, 48(9).
<https://doi.org/10.1029/2011WR011720>

- Harman, C. J. (2015). Time-variable transit time distributions and transport: Theory and application to storage-dependent transport of chloride in a watershed. *Water Resources Research*, 51(1), 1–30. <https://doi.org/10.1002/2014WR015707>
- Harvey, J., & Gooseff, M. (2015). River corridor science: Hydrologic exchange and ecological consequences from bedforms to basins. *Water Resources Research*, 51(9), 6893–6922. <https://doi.org/10.1002/2015WR017617>
- Hester, E. T., McEwen, A. M., Kim, B. J., & Rost, E. A. (2020). Abundance, distribution, and geometry of naturally occurring streambank soil pipes. *Freshwater Science*, 39(4), 735–751. <https://doi.org/10.1086/711655>
- Hewlett, J., & Hibbert, A. (1967). Factors Affecting the Response of Small Watersheds to Precipitation in Humid Areas. In *Proceedings of the International Symposium on Forest Hydrology*. Pergamon, Pennsylvania State University, NY.
- Hijmans, R. (2023). raster: Geographic Data Analysis and Modeling. Retrieved from <https://CRAN.R-project.org/package=raster>
- Hucks Sawyer, A., Bayani Cardenas, M., Bomar, A., & Mackey, M. (2009). Impact of dam operations on hyporheic exchange in the riparian zone of a regulated river. *Hydrological Processes*, 23(15), 2129–2137. <https://doi.org/10.1002/hyp.7324>
- Jaeger, K. L., Sutfin, N. A., Tooth, S., Michaelides, K., & Singer, M. (2017). Chapter 2.1 - Geomorphology and Sediment Regimes of Intermittent Rivers and Ephemeral Streams. In T. Datry, N. Bonada, & A. Boulton (Eds.), *Intermittent Rivers and Ephemeral Streams* (pp. 21–49). Academic Press. <https://doi.org/10.1016/B978-0-12-803835-2.00002-4>
- Jarvis, N., Koestel, J., & Larsbo, M. (2016). Understanding Preferential Flow in the Vadose Zone: Recent Advances and Future Prospects. *Vadose Zone Journal*, 15(12), vzj2016.09.0075. <https://doi.org/10.2136/vzj2016.09.0075>
- Jencso, K. G., McGlynn, B. L., Gooseff, M. N., Wondzell, S. M., Bencala, K. E., & Marshall, L. A. (2009). Hydrologic connectivity between landscapes and streams: Transferring reach- and plot-scale understanding to the catchment scale. *Water Resources Research*, 45(4). <https://doi.org/10.1029/2008WR007225>
- Jencso, K. G., & McGlynn, B. L. (2011). Hierarchical controls on runoff generation: Topographically driven hydrologic connectivity, geology, and vegetation. *Water Resources Research*, 47(11). <https://doi.org/10.1029/2011WR010666>

- Jones, C. N., Nelson, N. G., & Smith, L. L. (2019). Featured Collection Introduction: The Emerging Science of Aquatic System Connectivity I. *JAWRA Journal of the American Water Resources Association*, 55(2), 287–293. <https://doi.org/10.1111/1752-1688.12739>
- Jung, M., Burt, T. P., & Bates, P. D. (2004). Toward a conceptual model of floodplain water table response. *Water Resources Research*, 40(12). <https://doi.org/10.1029/2003WR002619>
- Junk, W., Bayley, P., & Sparks, R. (1989). The Flood Pulse Concept in River-Floodplain Systems. *Can. Spec. Public Fish. Aquat. Sci.* (Vol. 106).
- Kidd, R. E., & Lambeth, D. S. (1995). *Hydrogeology and ground-water quality in the Black Belt area of west-central Alabama, and estimated water use for aquaculture, 1990* (Water-Resources Investigations Report No. 94–4074). Tuscaloosa, Alabama: U.S. Geological Survey. Retrieved from https://web.archive.org/web/20190501065314id_/https://pubs.usgs.gov/wri/1994/4074/report.pdf
- Larned, S. T., Schmidt, J., Datry, T., Konrad, C. P., Dumas, J. K., & Diettrich, J. C. (2011). Longitudinal river ecohydrology: flow variation down the lengths of alluvial rivers. *Ecohydrology*, 4(4), 532–548. <https://doi.org/10.1002/eco.126>
- Larsen, L. G., Choi, J., Nungesser, M. K., & Harvey, J. W. (2012). Directional connectivity in hydrology and ecology. *Ecological Applications*, 22(8), 2204–2220. <https://doi.org/10.1890/11-1948.1>
- Laudon, H., & Sponseller, R. A. (2018). How landscape organization and scale shape catchment hydrology and biogeochemistry: insights from a long-term catchment study. *WIREs Water*, 5(2), e1265. <https://doi.org/10.1002/wat2.1265>
- Lee, E., Epstein, J. M., & Cohen, M. J. (2023). Patterns of Wetland Hydrologic Connectivity Across Coastal-Plain Wetlandscapes. *Water Resources Research*, 59(8), e2023WR034553. <https://doi.org/10.1029/2023WR034553>
- Leibowitz, S. G., Wigington Jr., P. J., Schofield, K. A., Alexander, L. C., Vanderhoof, M. K., & Golden, H. E. (2018). Connectivity of Streams and Wetlands to Downstream Waters: An Integrated Systems Framework. *JAWRA Journal of the American Water Resources Association*, 54(2), 298–322. <https://doi.org/10.1111/1752-1688.12631>

- Leigh, C., Sheldon, F., Kingsford, R. T., & Arthington, A. H. (2010). Sequential floods drive 'booms' and wetland persistence in dryland rivers: a synthesis. *Marine and Freshwater Research*, 61(8), 896–908. <https://doi.org/10.1071/MF10106>
- Loheide, S. P., & Booth, E. G. (2011). Effects of changing channel morphology on vegetation, groundwater, and soil moisture regimes in groundwater-dependent ecosystems. *Geomorphology*, 126(3), 364–376. <https://doi.org/10.1016/j.geomorph.2010.04.016>
- Loke, M. H., Chambers, J. E., Rucker, D. F., Kuras, O., & Wilkinson, P. B. (2013). Recent developments in the direct-current geoelectrical imaging method. *Journal of Applied Geophysics*, 95, 135–156. <https://doi.org/10.1016/j.jappgeo.2013.02.017>
- Lowe, W. H., & Likens, G. E. (2005). Moving Headwater Streams to the Head of the Class. *BioScience*, 55(3), 196. [https://doi.org/10.1641/0006-3568\(2005\)055\[0196:MHSTTH\]2.0.CO;2](https://doi.org/10.1641/0006-3568(2005)055[0196:MHSTTH]2.0.CO;2)
- Maloney, K. O., Feminella, J. W., Mitchell, R. M., Miller, S. A., Mulholland, P. J., & Houser, J. N. (2008). Landuse legacies and small streams: identifying relationships between historical land use and contemporary stream conditions. *Journal of the North American Benthological Society*, 27(2), 280–294. <https://doi.org/10.1899/07-070.1>
- McClain, M. E., Boyer, E. W., Dent, C. L., Gergel, S. E., Grimm, N. B., Groffman, P. M., et al. (2003). Biogeochemical Hot Spots and Hot Moments at the Interface of Terrestrial and Aquatic Ecosystems. *Ecosystems*, 6(4), 301–312. <https://doi.org/10.1007/s10021-003-0161-9>
- McDaniel, P. A., Regan, M. P., Brooks, E., Boll, J., Barndt, S., Falen, A., et al. (2008). Linking fragipans, perched water tables, and catchment-scale hydrological processes. *CATENA*, 73(2), 166–173. <https://doi.org/10.1016/j.catena.2007.05.011>
- McDonnell, J. J., Sivapalan, M., Vaché, K., Dunn, S., Grant, G., Haggerty, R., et al. (2007). Moving beyond heterogeneity and process complexity: A new vision for watershed hydrology. *Water Resources Research*, 43(7). <https://doi.org/10.1029/2006WR005467>
- McGlynn, B. L., & McDonnell, J. J. (2003). Quantifying the relative contributions of riparian and hillslope zones to catchment runoff. *Water Resources Research*, 39(11). <https://doi.org/10.1029/2003WR002091>

- McGuire, K., McDonnell, J., Weiler, M., Kendall, C., McGlynn, B., Welker, J., & Seibert, J. (2005). The role of topography on catchment-scale water residence time. *Water Resources Research*, 41. <https://doi.org/10.1029/2004WR003657>
- McLaughlin, D. L., Kaplan, D. A., & Cohen, M. J. (2014). A significant nexus: Geographically isolated wetlands influence landscape hydrology. *Water Resources Research*, 50(9), 7153–7166. <https://doi.org/10.1002/2013WR015002>
- McMillan, H., Araki, R., Gnan, S., Woods, R., & Wagener, T. (2023). How do hydrologists perceive watersheds? A survey and analysis of perceptual model figures for experimental watersheds. *Hydrological Processes*, 37(3), e14845. <https://doi.org/10.1002/hyp.14845>
- van der Meij, W. M., Temme, A. J. A. M., Lin, H. S., Gerke, H. H., & Sommer, M. (2018). On the role of hydrologic processes in soil and landscape evolution modeling: concepts, complications and partial solutions. *Earth-Science Reviews*, 185, 1088–1106. <https://doi.org/10.1016/j.earscirev.2018.09.001>
- Menéndez-Duarte, R., Marquínez, J., Fernández-Menéndez, S., & Santos, R. (2007). Incised channels and gully erosion in Northern Iberian Peninsula: Controls and geomorphic setting. *CATENA*, 71(2), 267–278. <https://doi.org/10.1016/j.catena.2007.01.002>
- Meyer, J. L., Strayer, D. L., Wallace, J. B., Eggert, S. L., Helfman, G. S., & Leonard, N. E. (2007). The Contribution of Headwater Streams to Biodiversity in River Networks¹. *JAWRA Journal of the American Water Resources Association*, 43(1), 86–103. <https://doi.org/10.1111/j.1752-1688.2007.00008.x>
- Miller, J., & Robinson, K. G. (1995). *A regional perspective of the physiographic provinces of the southeastern United States*.
- Montgomery, D. R. (1999). Process Domains and the River Continuum. *JAWRA Journal of the American Water Resources Association*, 35(2), 397–410. <https://doi.org/10.1111/j.1752-1688.1999.tb03598.x>
- Montgomery, D. R., & Dietrich, W. E. (1994). A physically based model for the topographic control on shallow landsliding. *Water Resources Research*, 30(4), 1153–1171. <https://doi.org/10.1029/93WR02979>
- Musolff, A., Fleckenstein, J. H., Rao, P. S. C., & Jawitz, J. W. (2017). Emergent archetype patterns of coupled hydrologic and biogeochemical responses in catchments. *Geophysical Research Letters*, 44(9), 4143–4151. <https://doi.org/10.1002/2017GL072630>

- Nadeau, T.-L., & Rains, M. C. (2007). Hydrological Connectivity Between Headwater Streams and Downstream Waters: How Science Can Inform Policy1. *JAWRA Journal of the American Water Resources Association*, 43(1), 118–133. <https://doi.org/10.1111/j.1752-1688.2007.00010.x>
- National Digital Elevation Program. (2021) LiDAR Elevation Dataset - Bare Earth DEM - 1 Meter (published 202106), accessed September, 2021 at <https://datagateway.nrcs.usda.gov/>
- Nimmo, J. R. (2012). Preferential flow occurs in unsaturated conditions. *Hydrological Processes*, 26(5), 786–789. <https://doi.org/10.1002/hyp.8380>
- Niswonger, R. G., & Fogg, G. E. (2008). Influence of perched groundwater on base flow. *Water Resources Research*, 44(3). <https://doi.org/10.1029/2007WR006160>
- NOAA National Centers for Environmental information. (2023). *Climate at a Glance: County Time Series*. Retrieved from <https://www.ncei.noaa.gov/access/monitoring/climate-at-a-glance/county/time-series>
- Osborne, W. E., Szabo, E. W., Copeland, C. W., & Neathery, T. L. (1988). *Geologic map of Alabama* (Special Map 220, scale 1:250,000). Geological Survey of Alabama. Retrieved from https://ngmdb.usgs.gov/Prodesc/proddesc_55859.htm
- Osborne, W. E., Szabo, E. W., Copeland, C. W., & Neathery, T. L. (1989). *Geologic map of Alabama* (Special Map 221, scale 1:500,000). Geological Survey of Alabama. Retrieved from https://ngmdb.usgs.gov/Prodesc/proddesc_55860.htm
- Pebesma, E. (2018). Simple Features for R: Standardized Support for Spatial Vector Data. *The R Journal*. 10(1), 439-446. <https://doi.org/10.32614/RJ-2018-009>
- Peterson, B. J., Wollheim, W. M., Mulholland, P. J., Webster, J. R., Meyer, J. L., Tank, J. L., et al. (2001). Control of Nitrogen Export from Watersheds by Headwater Streams. *Science*. <https://doi.org/10.1126/science.1056874>
- Plattner, A. M., Filoromo, S., & Blair, E. H. (2022). Multi-method geophysical investigation at Snow’s Bend, a Mississippian platform mound. *Archaeological Prospection*, 29(3), 343–351. <https://doi.org/10.1002/arp.1866>
- Poesen, J., Nachtergaele, J., Verstraeten, G., & Valentin, C. (2003). Gully erosion and environmental change: importance and research needs. *CATENA*, 50(2), 91–133. [https://doi.org/10.1016/S0341-8162\(02\)00143-1](https://doi.org/10.1016/S0341-8162(02)00143-1)

- Poff, N. L. (1997). Landscape Filters and Species Traits: Towards Mechanistic Understanding and Prediction in Stream Ecology. *Journal of the North American Benthological Society*, 16(2), 391–409. <https://doi.org/10.2307/1468026>
- Poole, G. C. (2010). Stream hydrogeomorphology as a physical science basis for advances in stream ecology. *Journal of the North American Benthological Society*, 29(1), 12–25. <https://doi.org/10.1899/08-070.1>
- Prancevic, J. P., & Kirchner, J. W. (2019). Topographic Controls on the Extension and Retraction of Flowing Streams. *Geophysical Research Letters*, 46(4), 2084–2092. <https://doi.org/10.1029/2018GL081799>
- Pringle, C. M. (2001). Hydrologic Connectivity and the Management of Biological Reserves: A Global Perspective. *Ecological Applications*, 11(4), 981–998. [https://doi.org/10.1890/1051-0761\(2001\)011\[0981:HCATMO\]2.0.CO;2](https://doi.org/10.1890/1051-0761(2001)011[0981:HCATMO]2.0.CO;2)
- R Core Team. (2023). R: A Language and Environment for Statistical Computing. Vienna, Austria: R Foundation for Statistical Computing. <https://www.R-project.org/>
- Raymond, D. E., Osborne, W. E., Copeland, C. W., & Neathery, T. L. (1988). *Stratigraphy of Alabama* (Circular 140). Geological Survey of Alabama.
- Richardson, J. S., & Danehy, R. J. (2007). A Synthesis of the Ecology of Headwater Streams and their Riparian Zones in Temperate Forests. *Forest Science*, 53(2), 131–147. <https://doi.org/10.1093/forestscience/53.2.131>
- Rinderer, M., Ali, G., & Larsen, L. G. (2018). Assessing structural, functional and effective hydrologic connectivity with brain neuroscience methods: State-of-the-art and research directions. *Earth-Science Reviews*, 178, 29–47. <https://doi.org/10.1016/j.earscirev.2018.01.009>
- Rücker, C., Günther, T., & Wagner, F. M. (2017). pyGIMLi: An open-source library for modelling and inversion in geophysics. *Computers & Geosciences*, 109, 106–123. <https://doi.org/10.1016/j.cageo.2017.07.011>
- Running, S., Mu, Q., Zhao, M., & Moreno, A. (2021). MODIS/Terra Net Evapotranspiration Gap-Filled Yearly L4 Global 500m SIN Grid V061 [Data set]. <https://doi.org/10.5067/MODIS/MOD16A3GF.061>
- Samad, M. A., Wodajo, L. T., Rad, P. B., Mamud, M. L., & Hickey, C. J. (2023). Integrated Agrogeophysical Approach for Investigating Soil Pipes in Agricultural Fields. *Journal of*

- Environmental and Engineering Geophysics*, 27(4), 207–217.
<https://doi.org/10.32389/JEEG22-007>
- Scaife, C. I., Singh, N. K., Emanuel, R. E., Miniati, C. F., & Band, L. E. (2020). Non-linear quickflow response as indicators of runoff generation mechanisms. *Hydrological Processes*, 34(13), 2949–2964. <https://doi.org/10.1002/hyp.13780>
- Schumm, S. A. (1977). *The fluvial system* (3rd ed). John Wiley and Sons, Inc.
- Shanafi, M., Bourke, S. A., Zimmer, M. A., & Costigan, K. H. (2021). An overview of the hydrology of non-perennial rivers and streams. *WIREs Water*, 8(2), e1504.
<https://doi.org/10.1002/wat2.1504>
- Shogren, A. J., Zarnetske, J. P., Abbott, B. W., Iannucci, F., Frei, R. J., Griffin, N. A., & Bowden, W. B. (2019). Revealing biogeochemical signatures of Arctic landscapes with river chemistry. *Scientific Reports*, 9(1), 12894. <https://doi.org/10.1038/s41598-019-49296-6>
- Sidle, R. C., & Onda, Y. (2004). Hydrogeomorphology: overview of an emerging science. *Hydrological Processes*, 18(4), 597–602. <https://doi.org/10.1002/hyp.1360>
- Simon, A., & Rinaldi, M. (2006). Disturbance, stream incision, and channel evolution: The roles of excess transport capacity and boundary materials in controlling channel response. *Geomorphology*, 79(3), 361–383. <https://doi.org/10.1016/j.geomorph.2006.06.037>
- Sivapalan, M. (2006). Pattern, Process and Function: Elements of a Unified Theory of Hydrology at the Catchment Scale. In *Encyclopedia of Hydrological Sciences*. John Wiley & Sons, Ltd. <https://doi.org/10.1002/0470848944.hsa012>
- Slater, L., & Lesmes, D. P. (2002). Electrical-hydraulic relationships observed for unconsolidated sediments. *Water Resources Research*, 38(10), 31-1-31–13.
<https://doi.org/10.1029/2001WR001075>
- Soil Survey Staff, Natural Resources Conservation Service, United States Department of Agriculture. Web Soil Survey. Accessed. June 2023. Available online
<https://websoilsurvey.nrcs.usda.gov/app/>
- Spence, C. (2010). A Paradigm Shift in Hydrology: Storage Thresholds Across Scales Influence Catchment Runoff Generation. *Geography Compass*, 4(7), 819–833.
<https://doi.org/10.1111/j.1749-8198.2010.00341.x>

- Squillace, P. J. (1996). Observed and Simulated Movement of Bank-Storage Water. *Groundwater*, 34(1), 121–134. <https://doi.org/10.1111/j.1745-6584.1996.tb01872.x>
- Swanson, J., Gregory, S., Sedell, J. R., & Campbell. (1982). Land-water interactions : The riparian zone. *Analysis of Coniferous Forest Ecosystems in the Western United States*, 267–291.
- Tetzlaff, D., Soulsby, C., Hrachowitz, M., & Speed, M. (2011). Relative influence of upland and lowland headwaters on the isotope hydrology and transit times of larger catchments. *Journal of Hydrology*, 400(3), 438–447. <https://doi.org/10.1016/j.jhydrol.2011.01.053>
- Tockner, K., Malard, F., & Ward, J. V. (2000). An extension of the flood pulse concept. *Hydrological Processes*, 14(16–17), 2861–2883. [https://doi.org/10.1002/1099-1085\(200011/12\)14:16/17<2861::AID-HYP124>3.0.CO;2-F](https://doi.org/10.1002/1099-1085(200011/12)14:16/17<2861::AID-HYP124>3.0.CO;2-F)
- Trancoso, R., Phinn, S., McVicar, T. R., Larsen, J. R., & McAlpine, C. A. (2017). Regional variation in streamflow drivers across a continental climatic gradient. *Ecohydrology*, 10(3), e1816. <https://doi.org/10.1002/eco.1816>
- Trimble, S. (1974). *Man-Induced Soil Erosion on the Piedmont*. Soil Conservation Society of America.
- Troch, P. A., Carrillo, G. A., Heidbüchel, I., Rajagopal, S., Switanek, M., Volkmann, T. H. M., & Yaeger, M. (2009). Dealing with Landscape Heterogeneity in Watershed Hydrology: A Review of Recent Progress toward New Hydrological Theory. *Geography Compass*, 3(1), 375–392. <https://doi.org/10.1111/j.1749-8198.2008.00186.x>
- Valentin, C., Poesen, J., & Li, Y. (2005). Gully erosion: Impacts, factors and control. *CATENA*, 63(2), 132–153. <https://doi.org/10.1016/j.catena.2005.06.001>
- Vanmaercke, M., Panagos, P., Vanwalleghem, T., Hayas, A., Foerster, S., Borrelli, P., et al. (2021). Measuring, modelling and managing gully erosion at large scales: A state of the art. *Earth-Science Reviews*, 218, 103637. <https://doi.org/10.1016/j.earscirev.2021.103637>
- Vannote, R. L., Minshall, G. W., Cummins, K. W., Sedell, J. R., & Cushing, C. E. (1980). The River Continuum Concept. *Canadian Journal of Fisheries and Aquatic Sciences*, 37(1), 130–137. <https://doi.org/10.1139/f80-017>
- Wainwright, H. M., Uhlemann, S., Franklin, M., Falco, N., Bouskill, N. J., Newcomer, M. E., et al. (2022). Watershed zonation through hillslope clustering for tractably quantifying

- above- and below-ground watershed heterogeneity and functions. *Hydrology and Earth System Sciences*, 26(2), 429–444. <https://doi.org/10.5194/hess-26-429-2022>
- Ward, J. V. (1989). The Four-Dimensional Nature of Lotic Ecosystems. *Journal of the North American Benthological Society*, 8(1), 2–8. <https://doi.org/10.2307/1467397>
- Warix, S. R., Navarre-Sitchler, A., Manning, A. H., & Singha, K. (2023). Local Topography and Streambed Hydraulic Conductivity Influence Riparian Groundwater Age and Groundwater-Surface Water Connection. *Water Resources Research*, 59(9), e2023WR035044. <https://doi.org/10.1029/2023WR035044>
- Wegener, P., Covino, T., & Wohl, E. (2017). Beaver-mediated lateral hydrologic connectivity, fluvial carbon and nutrient flux, and aquatic ecosystem metabolism. *Water Resources Research*, 53(6), 4606–4623. <https://doi.org/10.1002/2016WR019790>
- Weyman, D. R. (1973). Measurements of the downslope flow of water in a soil. *Journal of Hydrology*, 20(3), 267–288. [https://doi.org/10.1016/0022-1694\(73\)90065-6](https://doi.org/10.1016/0022-1694(73)90065-6)
- Willgoose, G., Bras, R. L., & Rodriguez-Iturbe, I. (1991). A coupled channel network growth and hillslope evolution model: 1. Theory. *Water Resources Research*, 27(7), 1671–1684. <https://doi.org/10.1029/91WR00935>
- Wilson, G. V., Neiber, J. L., Sidle, R. C., & Fox, G. A. (2013). Internal Erosion during Soil Pipeflow: State of the Science for Experimental and Numerical Analysis. *Transactions of the ASABE*, 56(2), 465–478.
- Winter, T. C. (1995). Recent advances in understanding the interaction of groundwater and surface water. *Reviews of Geophysics*, 33(S2), 985–994. <https://doi.org/10.1029/95RG00115>
- Winter, T. C. (1999). *Ground Water and Surface Water: A Single Resource*. DIANE Publishing.
- Wohl, E. (2006). Human impacts to mountain streams. *Geomorphology*, 79(3–4), 217–248. <https://doi.org/10.1016/j.geomorph.2006.06.020>
- Wohl, E., Brierley, G., Cadol, D., Coulthard, T. J., Covino, T., Fryirs, K. A., et al. (2019). Connectivity as an emergent property of geomorphic systems. *Earth Surface Processes and Landforms*, 44(1), 4–26. <https://doi.org/10.1002/esp.4434>
- Wu, Q., & Brown, A. (2022). whitebox: “WhiteboxTools” R Frontend. R package version 2.2.0. Retrieved from <https://CRAN.R-project.org/package=whitebox>

- Wymore, A. S., Ward, A. S., Wohl, E., & Harvey, J. W. (2023). Viewing river corridors through the lens of critical zone science. *Frontiers in Water*, 5. <https://doi.org/10.3389/frwa.2023.1147561>
- Yuval & Oldenburg, D. W. (1997) Computation of Cole-Cole parameters from IP data. *Geophysics*, 62 (2) 436-448. [doi:10.1190/1.1444154](https://doi.org/10.1190/1.1444154)
- Zimmer, M. A., & McGlynn, B. L. (2017). Ephemeral and intermittent runoff generation processes in a low relief, highly weathered catchment. *Water Resources Research*, 53(8), 7055–7077. <https://doi.org/10.1002/2016WR019742>
- Zimmer, M. A., & McGlynn, B. L. (2018). Lateral, Vertical, and Longitudinal Source Area Connectivity Drive Runoff and Carbon Export Across Watershed Scales. *Water Resources Research*, 54(3), 1576–1598. <https://doi.org/10.1002/2017WR021718>

Using Hydrogeomorphic Features to Quantify Structural and Functional Hydrologic Connectivity in a Coastal Plain Headwater Stream

Delaney M. Peterson¹, C. Nathan Jones¹, Alain M. Plattner², Ariel J. Shogren¹, and Sarah E. Godsey³

¹Department of Biological Sciences, University of Alabama, Tuscaloosa, AL, USA.

²Department of Geological Sciences, University of Alabama, Tuscaloosa, AL, USA.

³Department of Geosciences, Idaho State University, Pocatello, ID, USA.

Contents of this file

Text S1
Figure S1
Tables S1 to S3

Introduction

The following contains more detailed information about the study site (i.e., location; Text S1), study design, and additional data. The additional data include more detailed information about the soils described for the project, as well as where key horizons are located (Table S1). Additionally, it contains summary statistics of both the soils data (Table S2) and water table elevation data (Table S3) used in the manuscript. All elevation data was derived from field measurements and manually surveyed relative elevation. Soil horizon elevations were corrected by multiplying the measured horizon depth by the quotient of the measured total soil profile and the measured borehole depth.

Text S1.

The study watershed is a 0.9 km² forested site in Hale County, Alabama (USA). The watershed outlet is located at (32.851436, -87.663652), and drains a portion of the larger Tanglewood Biological Station before flowing into Fivemile Creek.

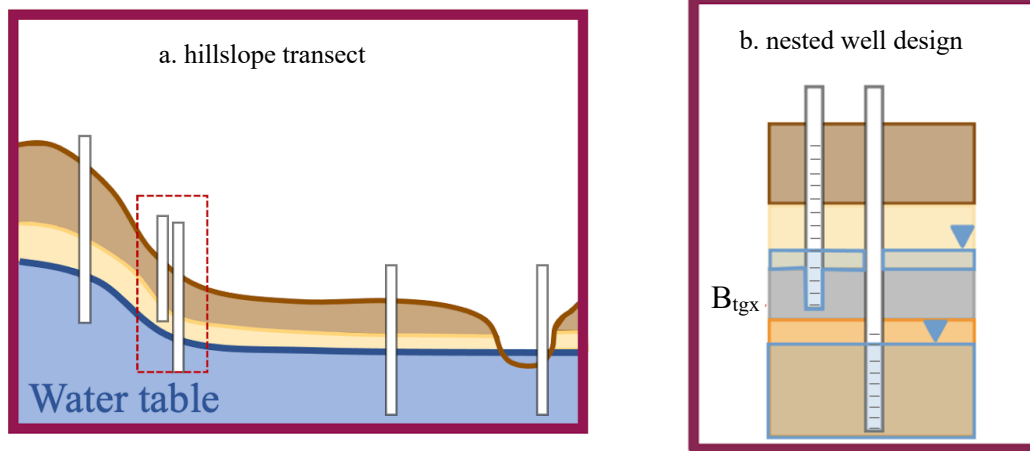


Figure S1. Site design for well installation. (a) shows the hillslope transect that was installed into each hydrogeomorphic feature, with one stream, one floodplain, a nested lower hillslope (indicated by the red dashed line), and one upper hillslope well. (b) shows the more detailed nested well design, with a shallow well screened from the argillic confining horizon (here, B_{tgx}) to within 10 cm of the ground surface. The deep well is screened from the bottom of the B_{tgx} to depths of refusal. Both the permanent deep and perched shallow water table are indicated in blue, showing that water level is higher in the shallow well (which reflects the discontinuous perched nature of the two zones of saturation).

Hydrogeomorphic Feature	Position	Horizon	Horizon Elevation (masl)	Horizon Depth (cm)
Incised	Upper Hillslope	A	64.40	8.9
		AB	64.31	9.4
		Bt1	64.22	31.9
		Bt2	63.90	85.0
		B1	63.05	28.9
		B2	62.76	12.4
		Bt3	62.64	97.4
		B3	61.66	10.0
		Bt4	61.56	43.1
		B4	61.13	32.5
		Bt5	60.81	20.7
		B5	60.60	115.7
		B6	59.44	20.1
		Bg1	59.24	14.8
		Bg2	59.10	18.9
		B7	58.91	20.7
		Bg3	58.70	23.6
		B8	58.46	15.9

		B9	58.30	10.6
		Bt6	58.20	8.9
	Lower Hillslope (Deep)	OA	59.97	5.5
		A	59.92	11.6
		AB	59.80	15.0
		B1	59.65	28.0
		B2	59.37	15.0
		Bt1	59.22	23.9
		B3	58.98	16.4
		B4	58.82	24.6
		B5	58.57	20.5
		Bt2	58.37	34.1
		Btgx1	58.02	38.2
		Btgx2	57.64	34.8
		Bt3	57.29	17.7
		B6	57.12	21.8
		Cg1	56.90	20.5
		Cg2	56.69	43.7
		Cg3	56.26	10.9

	Lower Hillslope (Shallow)	OA	59.97	5.5
		A	59.92	11.6
		AB	59.80	15.0
		B1	59.65	28.0
		B2	59.37	15.0
		Bt1	59.22	23.9
		B3	58.98	16.4
		B4	58.82	24.6
		B5	58.57	20.5
		Bt2	58.37	34.1
		Btgx1	58.02	38.2
		Btgx2	57.64	33.3
		Floodplain	A	56.80
	AB		56.76	7.2
	BE		56.69	18.3
	E		56.51	27.9
	Eg		56.23	51.8
	B		55.71	33.4
	Bg1		55.37	43.8

		Bg2	54.94	103.5
		Bt	53.90	19.1
		Btg1	53.71	22.3
		Btg2	53.49	17.5
		Btg3	53.31	34.2
Stream	Upper Hillslope	A	61.40	17.4
		Bt	61.23	37.0
		B1	60.86	65.0
		B2	60.21	57.5
		B3	59.63	34.0
		B4	59.29	15.9
		B5	59.13	34.0
		E	58.79	37.0
		EB	58.42	59.0
		B6	57.83	24.2
		Ob	57.59	6.0
		B7	57.53	23.4
		B8	57.29	15.1
		Btgx	57.14	14.4

	Lower Hillslope	A	55.00	5.9	
		Bt1	54.94	61.9	
		Bt2	54.32	18.4	
		Bt3	54.14	39.8	
		B1	53.74	53.0	
		B2	53.21	24.3	
		BE	52.97	49.4	
		B4	52.47	39.0	
		B5	52.08	50.8	
		Bg	51.57	43.5	
		Floodplain	A	51.99	5.8
	AB		51.93	8.1	
	Bt1		51.85	23.8	
	Bt2		51.61	40.0	
	Bt3		51.21	59.2	
	Bt4		50.62	8.1	
	Wetland	Upper Hillslope	A	59.10	16.0
			Bt	58.94	58.8
			B1	58.35	145.2

		B2	56.90	64.1
		B3	56.26	60.6
		B4	55.65	81.1
		B5	54.84	45.4
		BAb	54.39	74.8
		Ab	53.64	18.7
		B6	53.45	76.6
		Bg1	52.69	13.4
		Bg2	52.55	23.2
		Btg	52.32	7.1
		Lower Hillslope (Deep)	A	55.40
	Bt1		55.31	37.6
	BtO		54.93	15.2
	Ob		54.78	20.3
	E		54.58	14.5
	Ab		54.43	21.0
	AOb		54.22	11.6
	Ab2		54.10	15.9
	B1		53.95	12.3

		Btgx	53.82	13.0
		Bt2	53.69	10.9
		B2	53.58	19.5
		Bg1	53.39	24.6
		Bg2	53.14	15.9
		Cg	52.98	25.3
	Lower Hillslope (Shallow)	A	55.40	6.3
		Bt	55.34	46.8
		BOb	54.87	11.9
		Ob	54.75	25.4
		B1	54.50	70.6
		B2	53.79	34.9
		Btgx	53.44	3.2
	Floodplain	AO	51.20	14.3
		A	51.06	17.1
		AB	50.89	13.3
		B1	50.75	23.8
		BA	50.52	28.5
		B2	50.23	17.1

Table S1. Soils data from all boreholes. Each borehole contains all delineated horizons and their corresponding elevations (at the top of the horizon, masl) and depths (i.e., thickness, cm). Nested wells have the same horizons from the surface to the argillic confining horizon (here, B_{tgx}), and then the deep well includes the soil horizons below.

Hydrogeomorphic Feature	Position	Total Depth (m)	Percent Clay Horizon	Argillic Confining Horizon
Incised Channel	Upper Hillslope	6.29	45.6%	No
	Lower Hillslope (Deep)	3.82	38.9%	Yes
	Lower Hillslope (Shallow)	2.66	48.7%	Yes*
	Floodplain	3.83	24.3%	No
Intact Riparian Zone	Upper Hillslope	4.40	11.7%	Yes*
	Lower Hillslope	3.86	31.1%	No
	Floodplain	1.45	90.7%	No
Wetland-Stream Complex	Upper Hillslope	6.85	9.6%	No
	Lower Hillslope (Deep)	2.67	30.0%	Yes
	Lower Hillslope (Shallow)	1.99	25.1%	Yes*
	Floodplain	1.14	0%	No

Table S2. Soils summary information. Each borehole has an associated total depth (measured from the borehole, not from soils), the percentage of clay-dominated horizons, and whether there was an argillic confining horizon (here, B_{tgx}) present in the borehole.

* = well was screened above and into (> 10 cm) B_{tgx} horizon

Hydrogeomorphic Feature	Position	Mean WTE (m)	SD WTE (m)	CV (%)
Incised Channel	Upper Hillslope	58.4	0.156	0.27
	Lower Hillslope (Shallow)	57.7	0.144	0.25
	Lower Hillslope (Deep)	57.1	0.042	0.07
	Floodplain	54.8	0.179	0.33
	Stream	54.1	0.010	0.02
Intact Riparian Zone	Upper Hillslope	57.1*	0.009*	0.02*
	Lower Hillslope	52.1	0.040	0.08
	Floodplain	51.7	0.078	0.15
	Stream	52.0	0.027	0.05
Wetland	Upper Hillslope	55.3	0.101	0.18
	Lower Hillslope (Shallow)	53.9	0.052	0.10
	Lower Hillslope (Deep)	53.1	0.129	0.24
	Floodplain	51.1	0.056	0.11
	Stream	51.0	0.015	0.03

Table S3. Water Table Elevation (WTE) summary statistics. Each water monitoring well has a corresponding mean annual WTE (masl), as well as the standard deviation and coefficient of variation (CV).